

Estimates of critical loads and exceedances of acidity and nutrient nitrogen for mineral soils in Canada for 2014–2016 average annual sulphur and nitrogen atmospheric deposition

Hazel Cathcart¹, Julian Aherne², Michael D. Moran^{1*}, Verica Savic-Jovicic¹, Paul A. Makar¹, and Amanda Cole¹.

¹Air Quality Research Division, Atmospheric Science and Technology Directorate, Science and Technology Branch, Environment and Climate Change Canada, Toronto, Ontario, M3H 5T4, Canada

²School of the Environment, Trent University, Peterborough, Ontario, K9L 0G2, Canada

*Scientist emeritus

Correspondence to: Hazel Cathcart (hazel.cathcart@ec.gc.ca)

Abstract. The steady-state Simple Mass Balance model was applied to natural and semi-natural terrestrial ecosystems across Canada to produce nation-wide critical loads of acidity (maximum sulphur, CL_{maxS} ; maximum nitrogen, CL_{maxN} ; minimum nitrogen, CL_{minN}) and nutrient nitrogen (CL_{nutN}) at 250 m resolution. Parameterization of the model for Canadian ecosystems was considered with attention to the selection of the chemical criterion for damage at a site-specific resolution, with comparison between protection levels of 5% and 20% growth reduction (approximating commonly chosen base-cation-to-aluminum ratios of 1 and 10 respectively). Other parameters explored include modelled base cation deposition and site-specific nutrient and base cation uptake estimates based on North American tree chemistry data and tree species and biomass maps. Critical loads of acidity were estimated to be low (e.g., below 500 eq⁻¹ ha yr⁻¹) for much of the country, particularly above 60°N latitude where base cation weathering rates are low due to cold annual average temperature. Exceedances were mapped relative to annual sulphur and nitrogen deposition averaged over 2014–2016. Results show that under a conservative estimate (5% protection level), 10% of Canada's Protected and Conserved Areas in the study area experienced exceedance of some level of soil critical load of acidity while 70% experienced exceedance of soil critical load of nutrient nitrogen.

1 Introduction

During the last three decades, reductions in sulphur (S) and nitrogen (N) deposition have led to improvements in ecosystem health across the U.S. and Canada; nonetheless, the acid rain question remains relevant in Canada. Large point sources of emissions in western Canada have emerged, prompting concerns of impacts to sensitive ecosystems in British Columbia and the Athabasca Oil Sands Region (AOSR) in northeastern Alberta (e.g., Mongeon et al., 2010; Williston et al., 2016; Makar et al., 2018). Further, increased marine traffic in the Arctic due to the effects of anthropogenic warming has raised questions about potential impacts of acidic deposition on northern ecosystems already under pressure from climate change (Forsius et al., 2010; Liang and Aherne, 2019). Recovery of forest soils from decades of elevated acidic deposition in the northeastern U.S. and eastern Canada is encouraging, but is predicted to be slow (Lawrence et al., 2015; Hazlett et al., 2020) and is complicated by the effect of elevated N deposition (Clark

36 et al., 2013; Simkin et al., 2016; Pardo et al., 2019; Wilkins et al., 2023) and climate change (Wu and Driscoll, 2010).
37 The importance of N deposition to acidification and eutrophication has received increased recognition in recent years,
38 prompting new avenues of risk assessment and mapping (e.g. empirical critical loads of nitrogen; (Bobbink et al.,
39 2022; Bobbink and Hicks, 2014). While N oxide emissions in Canada declined by 41% between 1990 and 2022,
40 ammonia emissions increased by 24% in that same period (ECCC, 2024).

41
42 The critical loads concept, defined as “the maximum deposition that will not cause chemical changes leading to long-
43 term harmful effects on ecosystem structure and function” (Nilsson and Grenfelt, 1988) is the primary tool for
44 identifying ecosystems that are sensitive to air pollution, particularly with respect to acidification and eutrophication
45 (De Vries et al., 2015; Burns et al., 2008). Ecosystems that receive deposition above their critical load are said to be
46 in exceedance; that is, they are at risk of undergoing biological damage. Soil acidification is characterized by attrition
47 of base cations and a decrease in soil pH, which in turn causes leaching of toxic metals, such as aluminum, and damage
48 to plant roots. During the past three decades, these effects have been observed in forest soils in the northeastern U.S.
49 and eastern Canada (e.g., Cronan and Schofield, 1990; Likens et al., 1996; Lawrence et al., 1999) that received acidic
50 deposition in excess of their critical loads. The effects of nutrient N on ecosystems, which include eutrophication,
51 reduced plant biodiversity, and plant community changes, have also become an emerging issue, with studies
52 suggesting that some Canadian ecosystems are in exceedance of their nutrient N critical load (e.g., Aherne and Posch,
53 2013; Reinds et al., 2015; Williston et al., 2016).

54
55 The standard approach for estimating soil critical loads is the Simple Mass Balance (SMB) model (Sverdrup and De
56 Vries, 1994, Posch et al., 2015), a steady-state soil chemistry model with several simplifying assumptions to reduce
57 input requirements. This approach has been used for regional and provincial critical load assessments in Canada (e.g.,
58 Ouimet et al., 2006; Aklilu et al., 2022) as well as on a multi-provincial (NEG-ECP, 2001; Carou et al., 2008; Aherne
59 and Posch, 2013) and national scale (Reinds et al., 2015). However, nationwide implementations of the SMB model
60 in Canada have been challenged by data paucity and incompatibility across provinces (i.e. different data sources,
61 methodology and spatial alignment), coarse input map resolution, and computational difficulties driven by the size of
62 the country and the subsequent size of data files used in critical load calculations. In recent years, though, high-
63 resolution input data (for soils, meteorology, and forest composition) have become available and present an
64 opportunity to refine, expand, and harmonise critical loads across the entire country, including extending maps into
65 the Canadian Arctic. These developments come at a time when policymakers in Canada are seeking to define and
66 track air quality impacts (such as those by acidic S and N deposition) on sensitive ecosystems under the Addressing
67 Air Pollution Horizontal Initiative (ECCC, 2021). Furthermore, development of high-resolution critical loads of
68 nutrient N to assess terrestrial eutrophication risk may contribute to efforts to meet biodiversity goals such as those
69 under the Kunming-Montreal Global Biodiversity Framework (ECCC, 2023c). While the SMB model is a well-
70 established and widely used approach to determine critical loads, there remains a need for harmonised application
71 across Canadian ecosystems to provide maps from which the effects of S and N deposition can be assessed.

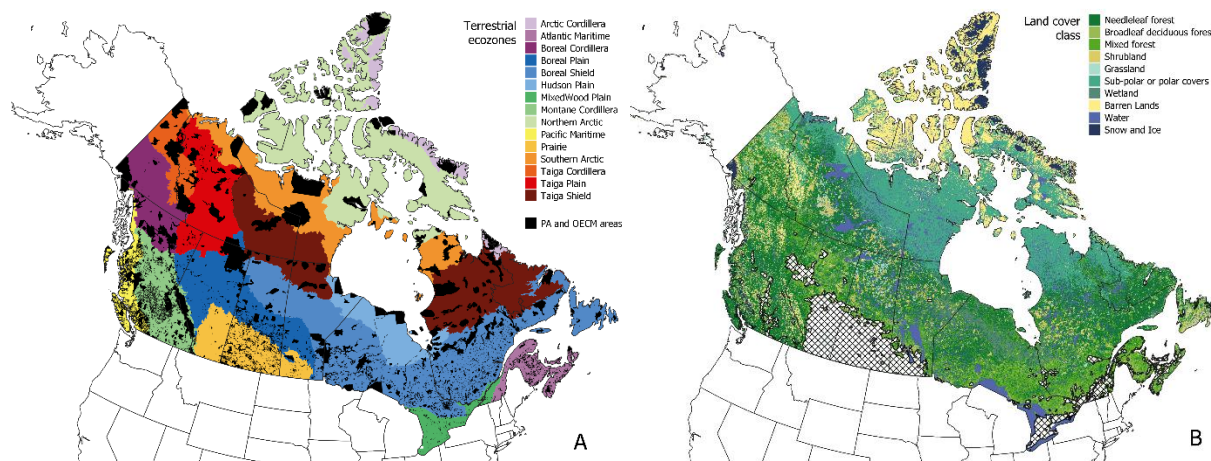
72

73 The objective of this study was to assess the impacts of acidic (S and N) and nutrient N deposition on terrestrial
74 ecosystems Canada-wide using the critical loads framework. In doing so, we applied a harmonised methodology to
75 the SMB model for Canadian ecosystems using high-resolution input maps, including modelled Canada-wide base
76 cation deposition (crucial for the estimation of critical loads). We also explored the choice of chemical (damage)
77 criteria for Canadian ecosystems using a site-specific approach. Finally, we assessed the impact of anthropogenic
78 base cation deposition on exceedance estimates under annual average S and N deposition (ECCC, 2023a) for the three-
79 year period 2014–2016, using the Canadian Protected and Conserved Areas Database (CPCAD; ECCC, 2023b), to
80 evaluate risk to sites that may be of interest to policymakers.

81 **2 Methods**

82 **2.1 Study area**

83 As the second-largest country by landmass in the world at over 9.9 million km², Canada is home to a variety of
84 climates, soils, vegetation, and geological structures that are grouped into distinct ecozones which are often used to
85 generalise critical loads across similar ecosystems (Figure 1A). The full extent of Canada was included in this study
86 to bring together estimates for all 10 provinces and 3 territories. However, only natural and semi-natural soils meeting
87 certain criteria for critical load estimations were considered. A land cover map (CEC, 2018) was used to exclude non-
88 soil ecosystems including water, wetlands, and permanent snow and ice (see Figure 1B). Soils were further limited
89 to natural and semi-natural ecosystems by excluding urban areas, crop classes, and areas within the boundaries of the
90 agricultural ecumene (Figure 1B). Areas considered “barren” by land classification were not excluded when mineral
91 soil depth was indicated in the interest of including as much of the Arctic region as possible; as the Arctic may be
92 greening under global climate change (Myers-Smith et al., 2020) and northern shipping routes become viable, the
93 question of ecosystem health in this region becomes more material. Since peat and wetland soil classification is
94 difficult at a Canada-wide scale (i.e., data at the required scale are presently unavailable), and given that the satellite
95 land cover map underestimates wetland cover (3.7% versus an expected 13% as given by the National Wetlands
96 Working Group; 1997), organic soils with 30% or more organic matter content were filtered out to close this gap. The
97 Hudson Plain ecozone, which contains the world’s largest contiguous wetland and is 80% wetland by cover (ECCC,
98 2016), was also broadly excluded from the study because of low mineral soil presence.

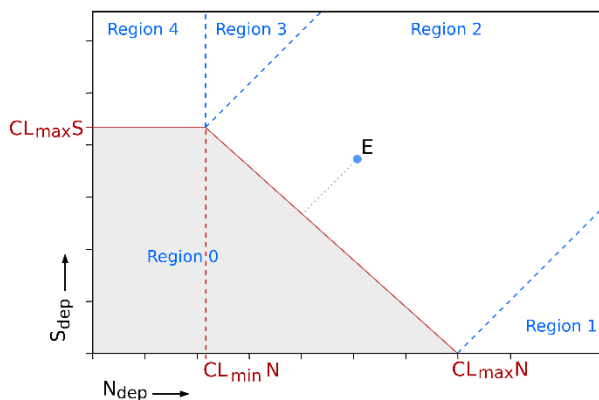


99 **Figure 1: Study area illustrating the 15 terrestrial eozones of Canada (A, data source: Agriculture and Agri-Food Canada,**
 100 **2013) with terrestrial Protected and Other Effective area-based Conservation Measures (OECM) areas in black (ECCC,**
 101 **2023b), as well as 15 (compressed to 9 for visualisation) land cover classes (B, data source: CEC, 2018) with agricultural**
 102 **regions in crosshatch (Statistics Canada, 2017).**

103

104 2.2 The Simple Mass Balance model for acidity and nutrient nitrogen

105 Critical loads of acidity were estimated using the SMB model, which balances sources, sinks, and outflows of S and
 106 N in terrestrial ecosystems while assuming ecosystems are at long-term equilibrium (i.e. about 100 years, representing
 107 at least one forest rotation cycle) (CLRTAP, 2015). The SMB model defines the critical load of S and N acidity
 108 (Figure 2) as a function of the maximum S critical load (CL_{maxS}), the maximum N critical load (CL_{maxN}), and the
 109 amount of N taken up by the ecosystem (CL_{minN}). Pairs of S and N deposition that fall outside this function (white
 110 area, Figure 2) signify that the receiving ecosystem is in exceedance of its critical load of acidity (i.e., it receives a
 111 potentially damaging amount of acidic deposition). Exceedance calculations are divided into four regions to determine
 112 the shortest path to the critical load line along the function.



113

114 **Figure 2: The acidity critical load function (red line) is defined by the maximum sulphur critical load (CL_{maxS}), the**
 115 **maximum nitrogen critical load (CL_{maxN}) and the minimum nitrogen critical load (CL_{minN}). Deposition points falling**
 116 **outside the critical load function (e.g., point E) are in exceedance (Regions 1-4), while those within the grey area (Region 0)**
 117 **are protected.**

118 The determination of $CL_{max}S$ requires knowledge of non-sea salt base cation (calcium, magnesium, potassium, sodium)
 119 deposition (BC_{dep}), soil base cation weathering (BC_{we}), chloride deposition (Cl_{dep}), base cation uptake (BC_{up}), and the
 120 critical leaching of Acid Neutralizing Capacity (the ability of the ecosystem to buffer incoming acidity), denoted
 121 $ANC_{le,crit}$ (see Eq. 1). Note that sodium is included in some base cation terms (denoted BC , e.g., BC_{we}) when sodium
 122 contributes to buffering, but where it concerns uptake by vegetation sodium is omitted since it is non-essential to
 123 plants (denoted Bc , e.g., Bc_{up}).

$$124 \quad CL_{max}S = BC_{dep} + BC_{we} - Cl_{dep} - Bc_{up} - ANC_{le,crit} \quad (1)$$

126
 127 The value of $ANC_{le,crit}$ (see Eq. 2) is determined from a critical base-cation-to-aluminum ratio (BC/Al_{crit}), which is set
 128 to protect the chosen biota within ecosystems of interest (i.e., the critical chemical criterion), soil percolation or runoff
 129 (Q), and the gibbsite equilibrium constant (K_{gibb} , see section 2.7).

$$130 \quad ANC_{le,crit} = -Q^{\frac{2}{3}} \cdot \left(1.5 \cdot \frac{BC_{dep} + BC_{we} - Bc_{up}}{K_{gibb} \cdot \left(\frac{BC}{Al}\right)_{crit}} \right)^{\frac{1}{3}} - \left(1.5 \cdot \frac{BC_{dep} + BC_{we} - Bc_{up}}{\left(\frac{BC}{Al}\right)_{crit}} \right) \quad (2)$$

132
 133 The calculation of $CL_{min}N$ from Eq. (3) describes the limit above which N deposition becomes acidifying, where N_u
 134 denotes N taken up by vegetation and N_i denotes long-term net immobilization of N in the root zone of soils under
 135 steady state conditions. A value of 35.7 eq ha⁻¹ yr⁻¹ (0.5 kg N ha⁻¹ yr⁻¹) was used, based on estimates of annual N_i
 136 since the last glaciation by Rosen et al. (1992) and Johnson and Turner (2014) who recommended a range of 0.2 – 0.5
 137 kg N ha⁻¹ yr⁻¹ and 0.5 – 1 kg N ha⁻¹ yr⁻¹ respectively; the midpoint (0.5 kg N ha⁻¹ yr⁻¹) was taken as a compromise.
 138 Lastly, $CL_{max}N$ is estimated from Eq. (4) using $CL_{max}S$, $CL_{min}N$, and the soil denitrification (the loss of nitrate to
 139 nitrogen gas) factor (f_{de} , see section 2.10).

$$140 \quad CL_{min}N = N_i + N_u \quad , \quad (3)$$

$$141 \quad CL_{max}N = CL_{min}N + \frac{CL_{max}S}{1-f_{de}} \quad . \quad (4)$$

142
 143
 144
 145 Equation (5) was used to estimate soil critical loads of nutrient N ($CL_{nut}N$), wherein the acceptable inorganic N
 146 leaching limit, a value set to prevent harmful effects of nutrient N such as eutrophication, vegetation community
 147 changes, nutrient imbalances, and plant sensitivity to stressors, is set from acceptable N concentrations in soil solution
 148 ($[N]_{acc}$) multiplied by Q (CLRTAP 2015). The $[N]_{acc}$ was set to 0.0142 eq m⁻³ (0.2 mg N l⁻¹ in soil solution) for conifer
 149 forests and 0.0214 eq m⁻³ (0.3 mg N l⁻¹) for all other semi-natural vegetation, following the generalised approach taken
 150 for the European critical loads database (Reinds et al., 2021) as values suggested in CLRTAP (2015) are often country-
 151 specific and do not extend to other regions or ecosystems.

152

$$153 \quad CL_{nut}N = N_i + N_{up} + \frac{Q*[N]_{acc}}{1-f_{de}} \quad . \quad (5)$$

154 **2.3 Data and mapping**

155 Critical load estimates were calculated with the statistical programming language R version 4.1.0 (R Core Team, 2021)
 156 and the Terra package (Hijmans, 2022) wherein inputs (Table 1) to and outputs from the SMB model were represented
 157 by 250 m resolution raster maps. Alignment and projection in the World Geodetic System (WGS84) followed the
 158 layers sourced from the OpenLandMap.org project (i.e., Hengl (2018c, a, d, b); Hengl and Wheeler (2018) in Table
 159 1), since they represented the majority of input (raster) data sources. Output maps were visualised using QGIS (QGIS
 160 Development Team, 2023) with accessible colour schemes (Tol, 2012). Acidity critical load components (CL_{maxS} ,
 161 CL_{maxN} , CL_{minN}) and $CL_{nut}N$ were all mapped using equivalents of acidity (or nutrient nitrogen) per hectare per year
 162 ($\text{eq ha}^{-1} \text{ yr}^{-1}$).

163

164 **Table 1: Data sources for input parameters to the SMB model and critical load exceedance calculation.**

Parameter	Units	Use	Original resolution	Source
Temperature				
Average annual air temperature (1981–2010)	°C	BC_{we}	250 m	McKenney et al., 2006
Soil				
Absolute depth to bedrock	cm	BC_{we}	250 m	Hengl, 2017
Organic carbon	$\times 5 \text{ g kg}^{-1}$	BC_{we}	250 m	Hengl & Wheeler, 2018
Sand fraction	%	BC_{we}	250 m	Hengl, 2018c
Clay fraction	%	BC_{we}	250 m	Hengl, 2018a
Bulk density	g/cm^3	BC_{we}	250 m	Hengl, 2018d
Coarse fragment volume	%	BC_{we}	250 m	Hengl, 2018b
Parent material acid class	class	BC_{we}	250 m	CLBBR, 1996; SLCWG, 2010
Drainage class	class	BC_{we}	250 m	CLBBR, 1996; SLCWG, 2010
Runoff (Q)	mm yr^{-1}	$ANC_{le,crit}$	$0.05^\circ \times 0.1^\circ$	Reinds et al., 2015
Vegetation				
Tree species composition	%	BC_{up} , N_{up}	250 m	Beaudoin et al., 2014
Biomass	Mg ha^{-1}	BC_{up} , N_{up}	250 m	Beaudoin et al., 2014
Harvestable boundaries	km^2	BC_{up} , N_{up}	250 m	Dymond et al., 2010
Tree chemistry database (U.S.)	% Ca, Mg, K, N	BC_{up} , N_{up}	-	Pardo et al., 2005
Tree chemistry database (Can.)	% Ca, Mg, K, N	BC_{up} , N_{up}	-	Paré et al., 2013
Land cover (2010)	class	Limiting extent	250 m	CEC, 2018
Agricultural ecumene (2016)	class	Limiting extent	5 km	Statistics Canada, 2017

Ecozones	class	Limiting extent, summary statistics	1:7.5 million	Agriculture and Agri-Food Canada, 2013
Deposition				
Base cation deposition (2010, 2016)	eq ha ⁻¹ yr ⁻¹	$ANC_{le,crit}$	12 km	Galmarini et al., 2021
Total mean S and N deposition (2014–2016)	eq ha ⁻¹ yr ⁻¹	Exceedance	10 km	Moran et al., 2024b, a
Canadian Protected and Conserved Areas Database	class	Identifying areas of special interest	Various	ECCC, 2023b

165

166 2.4 Base cation weathering

167 Base cation weathering BC_{we} (i.e., calcium, magnesium, potassium and sodium) was mapped using the soil type–
168 texture approximation method, which assigns a base cation weathering class (BC_{w0}) based on soil characteristics
169 (organic matter, sand, and clay percentage) and parent material acid class (see Eq. 6). A temperature correction was
170 applied to the BC_{we} as the speed of chemical weathering can be affected by temperature. Weathering is modified by
171 ambient temperature T , where A is the Arrhenius pre-exponential factor (3600 K), a temperature coefficient for soil
172 weathering (de Vries et al., 1992; CLRTAP, 2015). Note that average annual air temperature was used to approximate
173 annual average soil temperature in absence of a Canada-wide soil temperature map. To address issues with resolution
174 and continuity across provinces, high-resolution (global 250 m) predicted soil maps from the OpenLandMap.org
175 project were used for the following input variables: bulk density (ρ), organic carbon, coarse fragment volume (CF),
176 and sand and clay composition (see Table 1). One of the assumptions of the SMB model is that the soil compartment
177 is homogeneous; therefore, a weighted average for soil texture was developed based on layer depth, total depth (D),
178 and corrections based on coarse fragment volume, percent organic matter, and bulk density. Percent organic matter
179 (OM) was obtained by dividing organic carbon by 2 (Pribyl, 2010).

180

$$181 \quad BC_{we} = \left(\frac{\rho_{soil}}{\rho_{H_2O}} \right) D \left(1 - \frac{CF}{100} \right) \left(1 - \frac{OM}{100} \right) (BC_{w0} - 0.5) * 10^{\left(\frac{A}{281} - \frac{A}{273+T} \right)} \quad (6)$$

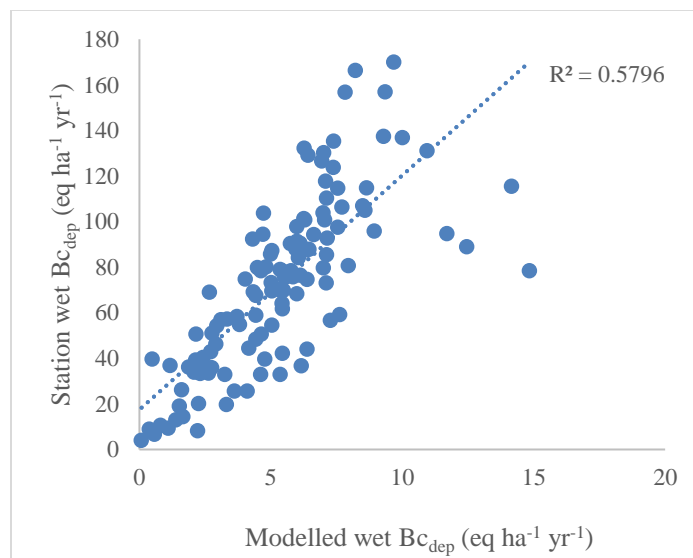
182

183 A second assumption is that the profile depth (D) is limited to the root zone, which was set to a maximum of 50 cm
184 for forest soils and 30 cm for other land cover types such as shrubland, grassland and tundra. Soil depth was further
185 limited by an absolute-depth-to-bedrock global modelled map (Hengl, 2017; Shangguan et al., 2017) in case bedrock
186 was < 50 cm. Base cation weathering omitting sodium (BC_{we}) required for the calculation of $ANC_{le,crit}$ (Eq. 2) was
187 scaled by 0.8 after CLRTAP (2015).

188 2.5 Base cation deposition

189 In the absence of modelled BC_{dep} data, previous Canadian mapping studies have employed a single value, or coarsely
190 interpolated from limited Canadian Air and Precipitation Monitoring Network (CAPMoN) stations from 1994–1998

191 (Aklilu et al., 2022; Carou et al., 2008; Ouimet et al., 2006). Critical loads estimates for Canada by Reinds et al.
 192 (2015) used coarse modelled global Ca deposition (Tegen and Fung, 1995) based on soil Ca content (Bouwman et al.,
 193 2002) and estimated the other ions by regression. To address the gaps in data availability and spatial distribution,
 194 BC_{dep} in this study was sourced from modelled estimates produced with the Global Environmental Multiscale–
 195 Modelling Air-quality and CHemistry (GEM-MACH) model at 12-km horizontal grid spacing for the air quality multi-
 196 model comparison project AQMEII4 (Galmarini et al., 2021). Two different GEM-MACH configurations, a version
 197 with detailed parameterizations and a second version with some simplified parameterizations used for operational air-
 198 quality forecast simulations, estimated wet and dry non-sea-salt BC_{dep} for North America. Gridded annual deposition
 199 fields for two periods, 2010 and 2016, were obtained. Ideally, emissions data sources used for S and N deposition and
 200 BC_{dep} would be the same; however, BC_{dep} is often not evaluated, and the version of the emissions inventories used for
 201 S and N deposition did not include BC_{dep} . In the absence of a modelled Cl_{dep} map, and since the model estimates non-
 202 marine BC_{dep} , Cl_{dep} was assumed to equal sodium deposition; BC_{dep} is therefore referred to as Bc_{dep} . Comparison of
 203 modelled wet Bc_{dep} to measured wet Bc_{dep} data from 33 Canadian Air and Precipitation Monitoring Network
 204 (CAPMoN) precipitation-chemistry stations (Feng et al., 2021) and 87 U.S. National Atmospheric Deposition
 205 Monitoring (NADP) precipitation-chemistry stations (NADP, 2023) within 300 km of the Canada-U.S. border showed
 206 that modelled Bc_{dep} data were underestimated in each model configuration and year by an average factor of 15, though
 207 the correlation was relatively high (Figure 3). A Bc_{dep} input map was prepared by averaging (wet plus dry) Bc_{dep}
 208 across the two model runs and two years, scaling up by 15 (after Figure 3), and resampling to the 250 m soil grid using
 209 bilinear interpolation.
 210



211
 212 **Figure 3: Modelled annual wet non-sea salt Bc_{dep} (Ca + Mg + K) versus measured annual Bc_{dep} at CAPMoN and NADP**
 213 **stations (NADP stations limited to those within 300 m of the Canada-U.S. border). Values are averaged across two years**
 214 **(2010 and 2016) and two model configurations. Marine station sites were corrected for sea salt contributions.**

215 The modelled Bc_{dep} and station observations include anthropogenic input, but the Bc_{dep} input to the SMB model is
 216 meant to reflect long-term non-anthropogenic sources of base cations. However, large point sources of Bc_{dep} (such as
 217 surface mines) are a feature of some Canadian regions, and their impact should not be overlooked in critical load

218 assessments. Pollutant Bc_{dep} from industrial sources can cause shifts in soil pH, plant community and biodiversity, as
219 well as direct damage to vegetation by dust (e.g. Mandre et al., 2008; Paal et al., 2013). To demonstrate the relative
220 impact of anthropogenic sources on Canadian critical loads estimates and to mitigate the impact anthropogenic local
221 Bc_{dep} inputs have in remote regions, two scenarios were assessed, one including anthropogenic Bc_{dep} and another that
222 attempted to smooth out anthropogenic “hot spots”.

223
224 To reduce the influence of anthropogenic point sources, a smoothing filter was applied using the SAGA GIS module
225 DTM Filter to identify local areas of locally intensified Bc_{dep} . Areas of Bc_{dep} above a 30% increase relative to a 20-
226 grid radius (approximately 50 km) were removed and infilled from their edges using inverse distance weighted
227 interpolation. Note that forest fire emissions may be substantial and appear as Bc_{dep} hot spots; for this application of
228 the SMB, we have not added a forest fire term to the base cation budget because of the difficulty of accounting forest
229 fire loss over the entire country. The loss of nitrogen due to forest fires from forest biomass and organic soil content
230 is also significant (and not reflected in N_{up} which only deals with loss from harvesting).

231 **2.6 Soil runoff**

232 Soil runoff was obtained from the hydrological model MetHyd (Bonten et al., 2016) following Reinds et al. (2015).
233 The data were resampled from the original resolution of $0.1 \times 0.05^\circ$ to 250 m and gaps were infilled from the edges.
234 A minimum Q was assigned ($10 \text{ m}^3 \text{ ha}^{-1} \text{ yr}^{-1}$) for broad regions where the coarse input soil map (FAO-UNESCO,
235 2003) used for hydrological modelling did not identify soil (i.e., exposed bedrock), but the high-resolution soil depth
236 and texture maps used for critical loads did identify soil.

237 **2.7 Gibbsite equilibrium constant**

238 The gibbsite equilibrium constant (K_{gibb}) describes the relationship between free (or unbound) aluminum concentration
239 and pH in the soil solution. As free aluminum concentrations are generally lower in the upper organic horizons,
240 observed ranges based on the organic matter content of the soil may be used to assign a K_{gibb} value. Soils with organic
241 matter less than 5% were assigned a value of $950 \text{ m}^6 \text{ eq}^{-2}$, soils with 5–15% organic matter were assigned a lower
242 value of $300 \text{ m}^6 \text{ eq}^{-2} \text{ yr}^{-1}$, and soils ranging from 15–30% organic matter were assigned a value of $100 \text{ m}^6 \text{ eq}^{-2}$ (after
243 CLRTAP, 2015).

244 **2.8 Chemical criterion for damage**

245 The critical base-cation-to-aluminum ratio (Bc/Al_{crit}) is the most widely used threshold, indicating damage to root
246 biomass. It is a simple approach that has been used in past Canadian estimates (e.g. Carou et al., 2008). In general,
247 it is applied as blanket or default value (e.g., $Bc/Al_{crit} = 1$) to a range of land cover types (e.g., forest or grassland). In
248 the current study, a species- and site-specific approach was used to assign damage thresholds for forest ecosystems
249 based on detailed tree species maps from the 2001 Canadian National Forest Inventory (NFI) (Beaudoin et al., 2014).
250 Two levels of protection were chosen to illustrate the difference between 20% acceptable growth reduction (generally
251 analogous to the default $Bc/Al_{crit} = 1$) versus a 5% growth reduction (generally analogous to $Bc/Al_{crit} = 10$). Dose-

252 response curves for Bc/Al_{crit} and root growth from Sverdrup and Warfvinge (1993) were matched to species present
 253 in the NFI database (Table 2). If forest was present above 25% coverage, values were sorted by the most sensitive
 254 tree species (those with the lowest Bc/Al_{crit}) above 5% species composition and given priority for the 250 m grid-cell
 255 value. If species-specific composition data for forests (from Beaudoin et al., 2014) were not available, the Bc/Al_{crit}
 256 value was averaged to the genus; if no genus-level data were available, an average coniferous, deciduous, or mixed
 257 forest value was applied. For non-forested soils, a default value based on a representative species for the land cover
 258 type was used (e.g., 4.5 and 0.8 for 5% and 20% protection levels, respectively, for grassland based on the response
 259 of *Deschampsia*).

260 **Table 2: Species-specific Bc/Al_{crit} values for 5% and 20% growth reduction following Sverdrup & Warfvinge (1993). Genus-**
 261 **level or generalised land cover values were derived from representative species.**

Category	Bc/Al_{crit} (mol/mol)	
	5%	20%
Species (forest)		
<i>Abies balsamea</i>	6.0	1.1
<i>Fagus grandifolia</i>	1.3	0.6
<i>Picea mariana</i>	2.5	0.8
<i>Pseudotsuga menzerii</i>	4.0	2.0
<i>Pinus strobus</i>	1.5	0.5
<i>Picea engelmannii</i>	2.5	0.5
<i>Pinus banksiana</i>	3.0	1.5
<i>Acer saccharum</i>	1.3	0.6
<i>Alnus glutinosa</i>	4.0	2.0
<i>Quercus rubra</i>	1.3	0.6
<i>Pinus ponderosa</i>	4.5	2.0
<i>Pinus resinosa</i>	4.5	2.0
<i>Picea rubens</i>	6.0	1.2
<i>Picea sitchensis</i>	2.5	0.4
<i>Larix laricina</i>	4.0	2.0
<i>Populus tremuloides</i>	8.0	4.0
<i>Tsuga heterophylla</i>	1.0	0.2
<i>Thuja plicata</i>	1.0	0.1
<i>Betula papyrifera</i>	4.0	2.0
<i>Picea glauca</i>	2.5	0.5
<i>Betula alleghaniensis</i>	4.0	2.0
<i>Betula populifolia</i>	4.0	2.0
<i>Picea abies</i>	6.0	1.2
<i>Pinus sylvestris</i>	3.0	1.2
Genus (forests)		
Abies	6.0	1.1
Acer	1.3	0.6
Alnus	4.0	2.0
Betula	4.0	2.0
Fagus	1.3	0.6
Larix	4.0	2.0
Picea	2.5	0.8
Pinus	3.0	1.5
Populus	8.0	4.0
Pseudotsuga	4.0	2.0
Quercus	1.3	0.6
Thuja	1.0	0.1
Tsuga	1.0	0.2

Generalised forest		
Deciduous	4.0	2.0
Coniferous	3.0	1.2
Mixed	3.0	1.2
Generalised land covers		
Grassland	4.5	0.8
Scrubland	2.8	0.6
Tundra	2.9	0.7

262

263 **2.9 Base cation and nitrogen uptake**

264 A species- and site-specific approach was also implemented to determine the net removal of nutrients (Ca, Mg, K, N)
 265 through tree harvesting from forest ecosystems. Base cation uptake ($B_{C_{up}}$) and N uptake (N_{up}) were estimated for
 266 forest soils by assuming stem-only removal; site-specific stand bark and trunk biomass estimates (Beaudoin et al.,
 267 2014) were multiplied by average trunk- and bark-specific nutrient and base cation concentration data from the tree
 268 chemistry databases for each species present. Two ‘tree chemistry’ databases were merged to include as many tree
 269 species as possible (U.S. data: Pardo et al., 2005; Canadian data: Paré et al., 2013); duplicate studies were removed
 270 from the merged database and species data were averaged across studies. A simplifying assumption was made that
 271 stand biomass was related to the species composition (i.e., the dominant tree species in a stand is also the dominant
 272 contributor to biomass). The nutrient uptake maps were restricted to harvestable forest areas as delineated by Dymond
 273 et al. (2010) and in all other regions it was set to 0. Nutrient uptake of other land types (e.g., grasslands) was considered
 274 negligible since grazing takes place primarily in agricultural regions, which have been broadly masked out. Since
 275 $B_{C_{up}}$ cannot exceed inputs from deposition, weathering, and losses from leaching, a scaling factor was used to constrain
 276 base cation uptake between its maximum (that is, deposition + weathering – leaching) and a minimum calcium
 277 leaching value. The same scaling factor was applied to N_{up} .

278 **2.10 Denitrification fraction**

279 The soil denitrification fraction (f_{de}) is generally related to soil drainage (CLRTAP, 2015); classes ranging from
 280 excessive to very poor drainage were assigned using the Canada-wide Canadian Soil Information Service (CanSIS)
 281 databases v2.2 (CLBBR, 1996) and v.3.2 (SLCWG, 2010). Because the databases are not compatible in their
 282 geographic extent and alignment, boundary and classification priority was given to the most recent database version
 283 before rasterization. Differences in classifications and their alignment to the soil drainage classes from CLRTAP
 284 (2015) are shown in Table 3.

285 **Table 3: Denitrification fraction (f_{de}) values (adapted from CLRTAP, 2015) and their corresponding drainage classifications**
 286 **in versions 2.2 and 3.2 of the Canadian Soil Information Service database.**

Drainage	f_{de}	V2.2	V3.2
Excessive	0	E/R	VR/R
Good	0.1	W	W
Moderate	0.2	M	MW

Imperfect	0.4	I	I
Poor	0.7	P	P
Very poor	0.8	V	VP

287

288 **2.11 Deposition and exceedance**

289 Exceedances for both acidity and nutrient nitrogen were calculated using total deposition maps of annual total S and
 290 N, which were sourced from GEM-MACH model output at 10 km horizontal grid spacing (GEM-MACH v3.1.1.0,
 291 RAQDPS version 023) (Moran et al., 2024a, b). A three-year (2014–2016) annual average was taken to reduce inter-
 292 annual variability in deposition, where input emissions based on annual emissions inventories specific to each of these
 293 three years were used for the three annual runs. Note that Moran et al. (2024b) have presented detailed evaluations of
 294 some components of these deposition estimates, specifically ambient concentration (as a proxy for dry deposition) and
 295 wet deposition of SO₂ and particle sulphate (p-SO₄), HNO₃ and p-NO₃, and NH₃ and p-NH₄, that suggest that they are
 296 robust.

297

298 Exceedances of critical load for both acidity and nutrient nitrogen (on a 250 m grid) were summarized to the 10 km
 299 deposition grid using Average Accumulated Exceedance (AAE), which is an area-weighted average that considers
 300 ecosystem coverage within each grid cell to derive the average of the summed exceedance; this addresses issues with
 301 sparse coverage and considers all ecosystems within the grid (Posch et al., 1999). The Canadian Protected and
 302 Conserved Areas Database (CPCAD) was used to identify areas in exceedance that may be of particular concern to
 303 policymakers (ECCC, 2023b). The database, assembled in support of Canada’s reporting on Canadian Environmental
 304 Sustainability Indicators and the UN Convention on Biological Diversity (among other initiatives), identifies Protected
 305 Areas (PA) such as national and provincial parks as well as Other Effective area-based Conservation Measures
 306 (OECM). Interim areas were included in expectation of their formal establishment. Areas that fell entirely within the
 307 agricultural ecumene were removed, but areas that straddled the ecumene were retained. Areas were counted as in
 308 exceedance if any part of the area experienced exceedance at the 250 m resolution.

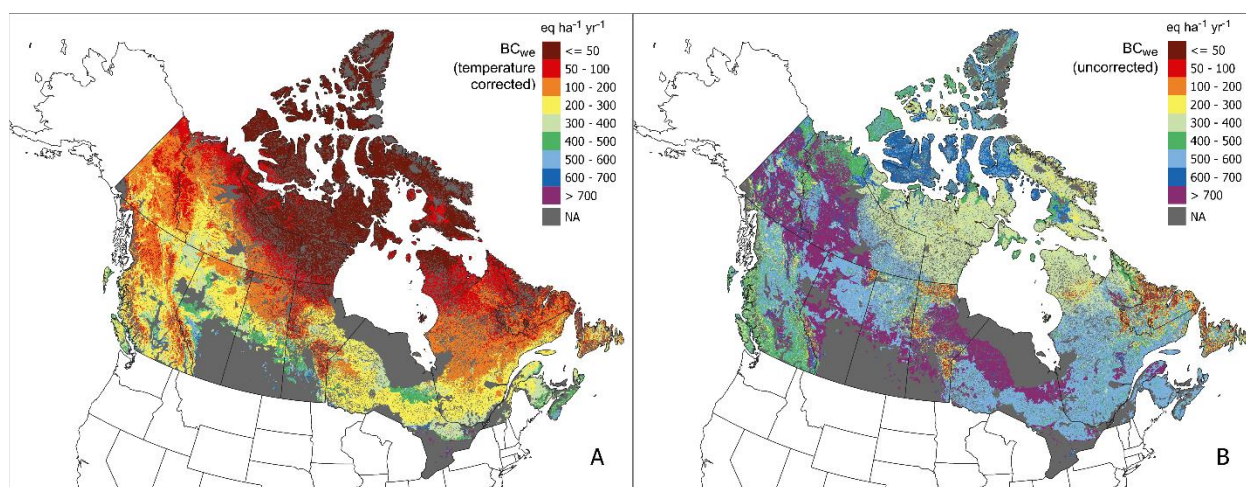
309

310 The exceedance calculations used for acidity employed the methodology described by Posch et al. (2015), where the
 311 critical load function (Figure 2) was divided into five regions, and a different formula for exceedance was used for
 312 each region. Five inputs for each 250 m grid cell were required for these calculations: the S and N total deposition
 313 pair plus $CL_{max}S$, $CL_{min}N$, and $CL_{max}N$ values. For S and N total deposition pairs falling into four of the regions, the
 314 exceedance value will be positive (i.e., in exceedance) and its magnitude indicates how great the S and N acidic
 315 deposition at the location is above the critical load for acidity. For the Region 0, the exceedance value will be negative
 316 (i.e., not in exceedance) and its magnitude will give how far the S and N acidic deposition is below the critical load
 317 for acidity. Calculation of nutrient N exceedance was simply the difference between N_{dep} and $CL_{nut}N$.

318 **3 Results**

319 **3.1 Base cation weathering**

320 The estimated BC_{we} was very low (below $100 \text{ eq ha}^{-1} \text{ yr}^{-1}$) for nearly all regions north of 60°N latitude, and low (below
 321 $200 \text{ eq ha}^{-1} \text{ yr}^{-1}$) for many northern regions south of 60°N latitude (Figure 4A). Higher BC_{we} (above $500 \text{ eq ha}^{-1} \text{ yr}^{-1}$)
 322 was predicted for the calcareous and deep soils of the Prairies and southern Ontario adjacent to agricultural regions
 323 (i.e. the mean Prairie average for natural and semi-natural soils was $714 \text{ eq ha}^{-1} \text{ yr}^{-1}$), although most of these ecozones
 324 are excluded as part of the agricultural ecumene (Table 4). Average BC_{we} for the Arctic ecozones was $< 50 \text{ eq ha}^{-1} \text{ yr}^{-1}$,
 325 in contrast with $BC_{we} > 700$ for Mixed Wood Plain and Prairie ecozones. Similarly, provincial averages were lowest
 326 for Nunavut and highest for Saskatchewan (Table 4). Base cation weathering without temperature correction (Figure
 327 4B, mean value of $570 \text{ eq ha}^{-1} \text{ yr}^{-1}$) illustrates the strong effect temperature has on limiting BC_{we} in most of the country
 328 (average $173 \text{ eq ha}^{-1} \text{ yr}^{-1}$), particularly Arctic and mountainous regions.
 329



330
 331 **Figure 4: Base cation weathering rate (Ca+Mg+K+Na) with temperature correction (A) and without (B). The weathering**
 332 **rate was estimated using a soil texture approximation method with sand, clay, and parent material acid class modified by**
 333 **depth (see Section 2.4).**

334 **Table 4: Ecozone and provincial mean values for inputs and outputs of the Simple Mass Balance model, including base**
 335 **cation weathering (BC_{we}), smoothed base cation deposition (BC_{dep}), base cation uptake (BC_{up}), nitrogen uptake (N_{up}), critical**
 336 **base-cation-to-aluminum ratio (Bc/Al_{crit}) for 5% and 20% growth reductions, average sulphur deposition ($DepS$) and**
 337 **nitrogen deposition ($DepN$) 2014 - 2017, maximum critical load of sulphur (CL_{maxS}), maximum critical load of nitrogen**
 338 **(CL_{maxN}), minimum nitrogen critical load (CL_{minN}) and critical load of nutrient nitrogen (CL_{nutN}). Units are in $\text{eq ha}^{-1} \text{ yr}^{-1}$**
 339 **except for Bc/Al_{crit} which is a unitless ratio. The critical loads presented in the table were calculated using the 5% Bc/Al_{crit}**
 340 **and the smoothed BC_{dep} . Note that values represent averages over eligible soils (e.g. excluding agricultural areas and organic**
 341 **soils).**

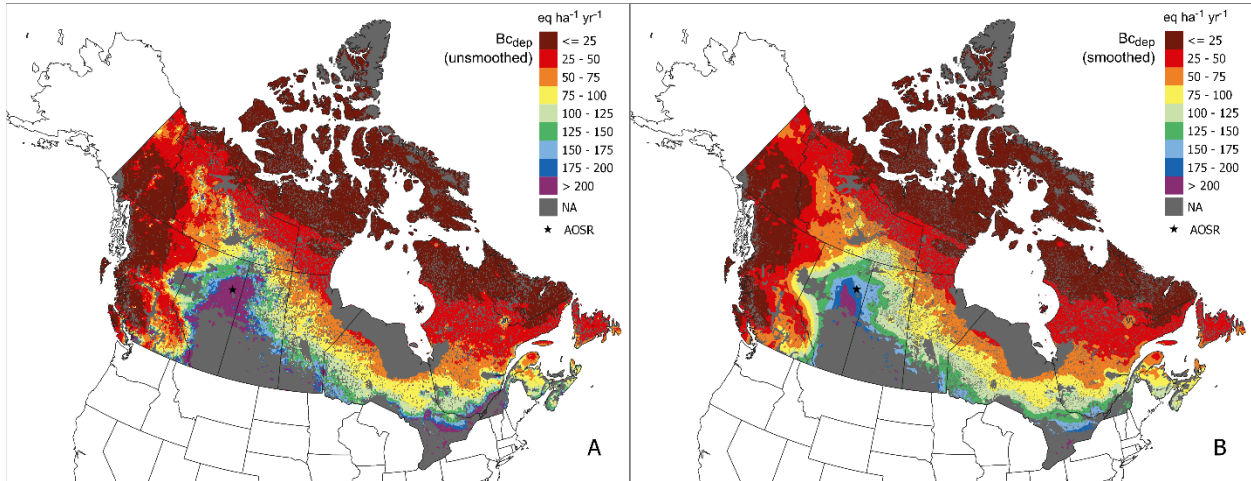
Ecozone	BC_{we}	BC_{dep}	BC_{up}	N_{up}	Bc/Al_{crit} 5%	Bc/Al_{crit} 20%	$DepS$	$DepN$	CL_{max} S	CL_{max} N	CL_{min} N	CL_{nut} N
Arctic Cordillera	40	5	< 1	< 1	5.2	1.2	8	21	82	88	36	173
Atlantic Maritime	353	89	32	37	5.7	1.1	57	240	615	551	36	234
Boreal Cordillera	174	19	5	5	3.9	1.2	10	29	290	274	36	77
Boreal Plain	331	139	27	23	3.7	1.4	38	172	802	549	36	71

Boreal Shield	229	84	18	23	4.0	0.9	53	206	512	422	36	147
Mixedwood Plain	712	180	< 1	< 1	3.6	0.9	137	712	1586	1171	36	145
Montane Cordillera	240	52	39	42	3.6	1.2	25	98	447	473	40	164
Northern Arctic	32	7	< 1	< 1	5.6	1.3	9	20	63	75	41	75
Pacific Maritime	274	25	78	135	2.9	0.9	53	172	608	1281	48	513
Prairie	559	191	13	2	5.0	1.9	54	423	1078	893	59	63
Southern Arctic	45	21	< 1	< 1	5.6	1.3	10	26	112	118	60	65
Taiga Cordillera	106	31	< 1	< 1	4.3	1.0	10	26	218	194	76	66
Taiga Plain	195	51	4	4	3.2	1.0	13	37	390	246	79	51
Taiga Shield	88	40	< 1	< 1	3.5	0.8	18	54	227	200	192	110
Province												
Alberta	285	133	24	17	3.7	1.4	35	142	730	512	58	78
British Columbia	235	37	40	53	3.6	1.2	26	92	439	551	91	206
Manitoba	217	86	7	7	2.9	0.9	41	146	512	338	44	66
New Brunswick	344	91	34	41	5.8	1.1	49	227	595	502	79	243
Newfoundland & Labrador	110	24	6	7	4.6	0.9	24	71	217	190	43	223
Nova Scotia	422	92	21	28	5.6	1.1	68	249	733	652	65	261
Northwest Territories	114	41	< 1	< 1	4.0	1.0	11	28	254	191	36	49
Nunavut	34	11	< 1	< 1	5.5	1.2	9	22	75	87	36	75
Ontario	306	103	23	19	3.8	0.9	61	289	666	509	66	141
Prince Edward Island	422	69	19	18	5.3	1.0	57	209	672	558	66	226
Québec	148	46	11	14	4.5	1.0	38	132	314	299	50	153
Saskatchewan	230	124	12	8	3.1	1.0	29	128	607	492	49	62
Yukon	148	25	< 1	< 1	3.8	1.0	10	26	266	233	36	54
Canada	132	52	8.2	10	4.5	1.1	76	22	291	258	48	99

342 3.2 Base cation deposition

343 Modelled BC_{dep} ranged from low ($< 25 \text{ eq ha}^{-1} \text{ yr}^{-1}$) in the north to higher values ($> 200 \text{ eq ha}^{-1} \text{ yr}^{-1}$) around the Prairies
344 and the southern regions of the eastern provinces (Figure 5) as well as in Alberta and Saskatchewan (Table 4). Average
345 (smoothed) BC_{dep} was roughly one-third of BC_{we} . Hot spots of BC_{dep} associated with anthropogenic point sources
346 (e.g., from mining operations as well as the contribution from the AOSR) were clearly visible in the unsmoothed map
347 (Figure 5A). The smoothing algorithm (Figure 5B) eliminated most of the effects of point sources, at the cost of
348 lowering average BC_{dep} (Canada-wide average of $68 \text{ eq ha}^{-1} \text{ yr}^{-1}$ pre-smoothing and $52 \text{ eq ha}^{-1} \text{ yr}^{-1}$ post-smoothing).
349 However, it did not completely erase elevated BC_{dep} in the AOSR; the difference in size between other point source

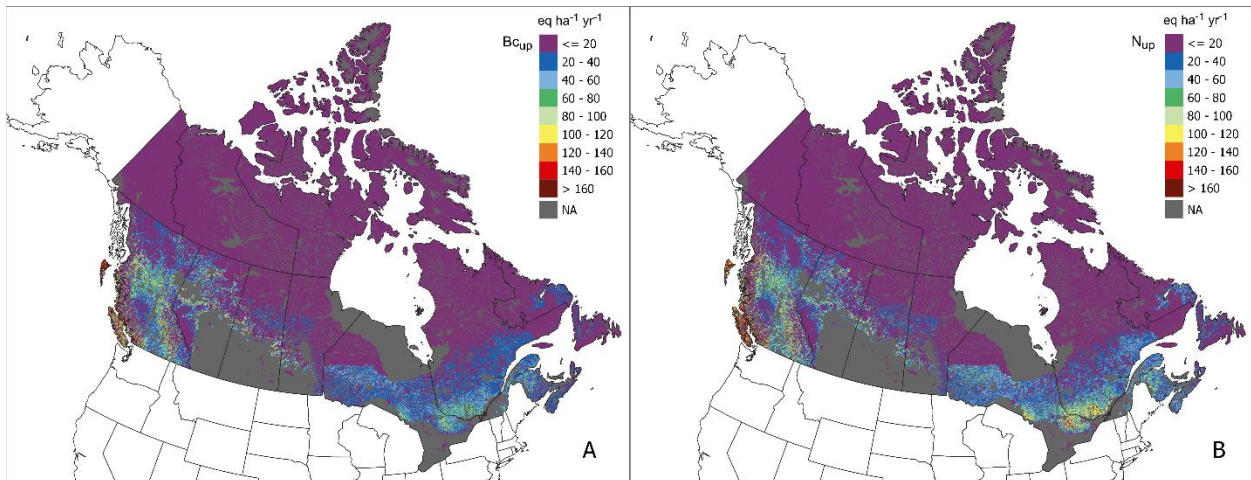
350 footprints and the AOSR necessitated a compromise in filter radius and slope selection. The smoothed Bc_{dep} was
 351 adopted as the primary data set for presenting the critical loads.



352
 353 **Figure 5: Non-sea-salt base cation deposition (Ca + Mg + K) with anthropogenic contributions (A) and after a smoothing**
 354 **filter was applied to reduce the effect of anthropogenic point sources (B). The location of the city of Fort McMurray within**
 355 **the Athabasca Oil Sands Region (AOSR) is identified by a star.**

356 3.3 Base cation and nitrogen uptake

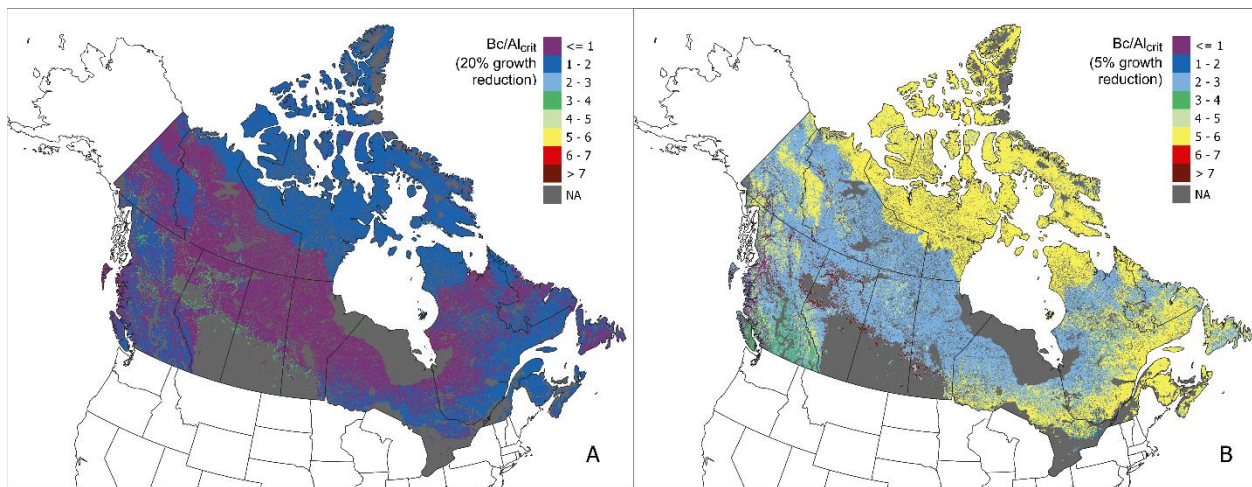
357 Base cation uptake ranged from < 1 to $545 \text{ eq ha}^{-1} \text{ yr}^{-1}$ and was highest in coastal British Columbia; the Pacific
 358 Maritime ecozone had the highest mean Bc_{up} at $79 \text{ eq ha}^{-1} \text{ yr}^{-1}$ (Table 4). Nitrogen uptake was also high in British
 359 Columbia and the Pacific Maritime zone (mean N_{up} of $135 \text{ eq ha}^{-1} \text{ yr}^{-1}$) as well as the Montane Cordillera (mean N_{up}
 360 of $42 \text{ eq ha}^{-1} \text{ yr}^{-1}$). Regions of elevated N_{up} were seen in eastern Ontario and southern Quebec (Figure 6); these occur
 361 on the Boreal Shield ecozone, which is a large ecozone that extends across multiple provinces over which N_{up} varies
 362 (but with a mean value of $23 \text{ eq ha}^{-1} \text{ yr}^{-1}$).



363
 364 **Figure 6: Base cation (Ca+Mg+K) uptake (A) and nitrogen uptake (B); forested regions limited to harvestable regions**
 365 **(identified by Dymond et al. (2010)). Uptake for non-forested ecosystems was set to 0.**

366 3.4 Critical base-cation-to-aluminum ratio

367 Almost the entire country fell below a Bc/Al_{crit} ratio of 2 under 20% root biomass growth reduction (Figure 7A). In
368 contrast, a Bc/Al_{crit} ranged from 1–8 (average = 4.4) under the 5% root biomass growth reduction (Figure 7B). The
369 ratio ranged from 3–6 for forests in eastern Canada (A and B ecozones), while ranges for the Boreal Shield ecozone
370 were 2–4 and coastal forest in British Columbia were slightly higher at 3–4. Semi-natural grassland in the Prairies
371 were given a ratio of 4.5 based on *Deschampsia*, but many fringe regions of the Prairies are treed and dominated by
372 *Populus tremuloides*, which had a Bc/Al_{crit} of 8.

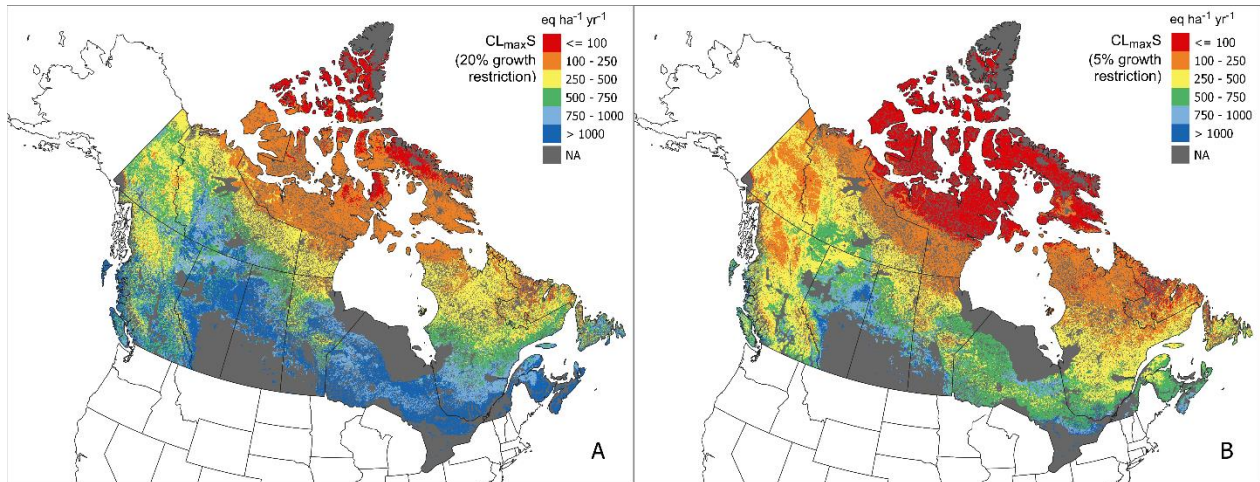


373
374 **Figure 7: Critical base-cation-to-aluminum ratio (Bc/Al_{crit}) under a 20% growth reduction (A) and a 5% growth reduction**
375 **(B). Site-specific ratios were selected for each 250 m grid cell for the most sensitive species (or genus or land-cover type if**
376 **no species data available). Note that while the legends have been matched for comparison, the maximum ratio in the 20%**
377 **growth reduction map is 4.**

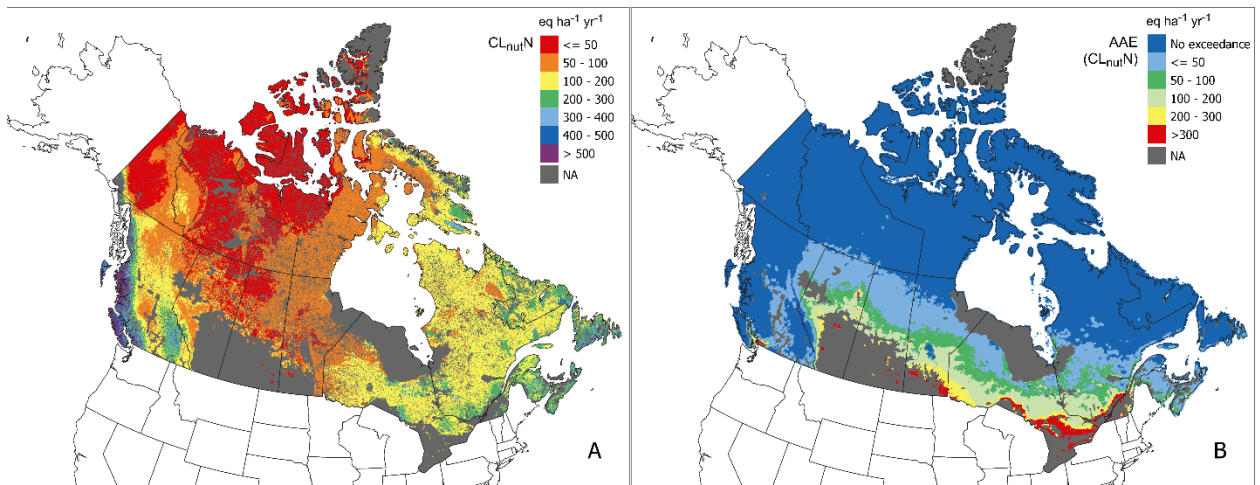
378 3.5 Critical loads

379 The CL_{maxS} under the 20% protection level (i.e., allowing more damage) showed low sensitivity ($> 1000 \text{ eq ha}^{-1} \text{ yr}^{-1}$)
380 to acidic deposition for most regions below 55°N latitude (Figure 8A). In contrast, under the 5% protection level
381 (Figure 8B), low sensitivity was limited to southern agricultural regions in the Prairies. Lowest CL_{maxS} and CL_{maxN}
382 were found in the Arctic territories (Nunavut, the Northwest Territories, the Yukon; Table 4) and also Newfoundland
383 and Labrador. Of the provinces, Quebec had the lowest CL_{maxS} ($314 \text{ eq ha}^{-1} \text{ yr}^{-1}$) and CL_{maxN} ($299 \text{ eq ha}^{-1} \text{ yr}^{-1}$) (Table
384 4). From an ecozone perspective the Mixedwood Plain ecozone had the highest CL_{maxS} at $1586 \text{ eq ha}^{-1} \text{ yr}^{-1}$ followed
385 by the Prairies at $1078 \text{ eq ha}^{-1} \text{ yr}^{-1}$. The most sensitive ecozones outside the Arctic ecozones (which were below 100
386 $\text{eq ha}^{-1} \text{ yr}^{-1}$) were the Boreal Cordillera and the Taiga ecozones (Table 4). For CL_{nutN} , central and northern regions of
387 the country were sensitive to nutrient N deposition, particularly pastures, grasslands, scrublands, and sparse forest in
388 and surrounding the Prairies (Figure 9A). Further, very low CL_{nutN} ($\leq 75 \text{ eq ha}^{-1} \text{ yr}^{-1}$) were estimated over the Arctic
389 territories (Table 4) as well as in northern Alberta and the Athabasca Basin in northern Saskatchewan. The coastal
390 ecozones had the highest CL_{nutN} , with the Pacific and Atlantic Maritime zones having 513 and $235 \text{ eq ha}^{-1} \text{ yr}^{-1}$
391 respectively. The Prairie ecozone had the lowest CL_{nutN} , lower than some of the Arctic ecozones, at $63 \text{ eq ha}^{-1} \text{ yr}^{-1}$.

392



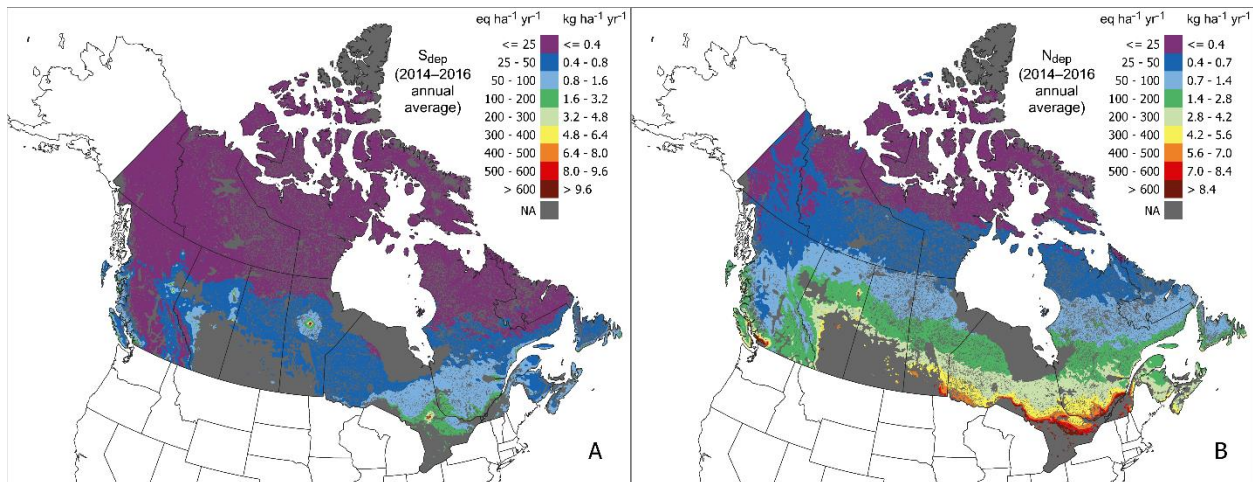
393
 394 **Figure 8: Maximum sulphur critical load (CL_{maxS}) at a 20% growth restriction scenario (A) versus a 5% growth restriction**
 395 **scenario (B), using reduced-anthropogenic (i.e., smoothed) BC_{dep} .**



396
 397 **Figure 9: Critical load of nutrient nitrogen using the SMB model (A) and average accumulated exceedance of nutrient**
 398 **nitrogen (B) estimated under modelled total deposition of nitrogen from 2014–2016.**

399 3.6 Deposition

400 Modelled average annual S_{dep} was below $25 \text{ eq ha}^{-1} \text{ yr}^{-1}$ for most of the country above 59°N , as well as the Montaine
 401 Cordillera ecozone that covers much of British Columbia (Figure 10A). Southern Quebec and central Ontario showed
 402 higher annual average values between $50\text{--}200 \text{ eq ha}^{-1} \text{ yr}^{-1}$, with some point sources showing S_{dep} in excess of 500 eq
 403 $\text{ha}^{-1} \text{ yr}^{-1}$ (e.g., at nickel smelters and mining operations in Sudbury, Ontario and Thompson, Manitoba). Modelled
 404 average annual N_{dep} (Figure 9B) exceeded S_{dep} in most parts of the country. A north-south N_{dep} gradient is observable
 405 in Figure 10B, showing higher N_{dep} closer to agricultural sources in southern Ontario and Quebec and in the Prairies.
 406 Nitrogen deposition exceeding $500 \text{ eq ha}^{-1} \text{ yr}^{-1}$ was present in northern Ontario and southern Quebec as well as
 407 southern Manitoba and southwestern British Columbia.



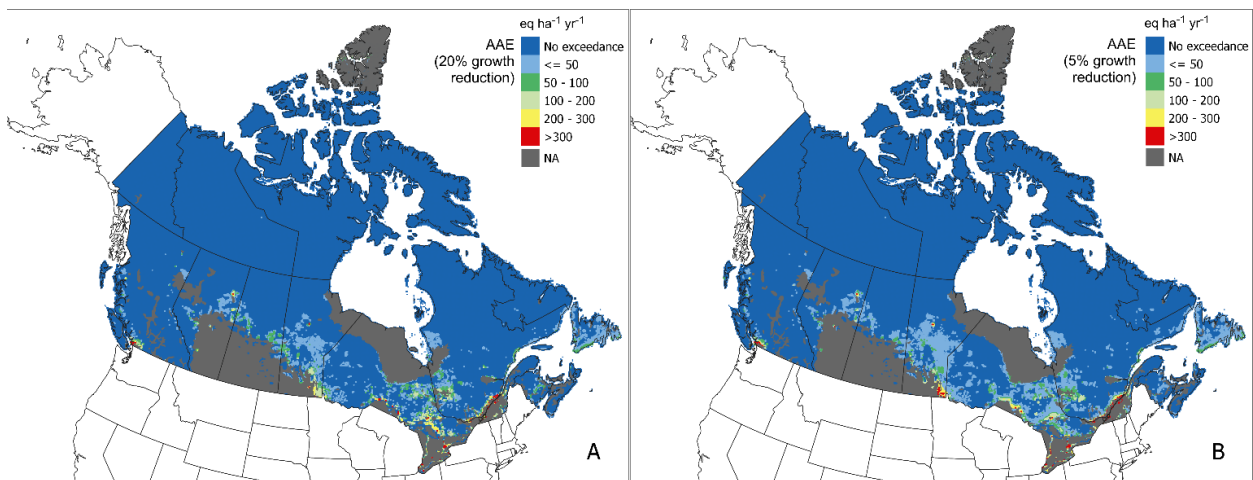
408
 409 **Figure 10: Modelled annual average (2014–2016) total deposition of sulphur (S_{dep} , panel A) and nitrogen (N_{dep} , panel B).**
 410 **Maps were sourced from GEM-MACH (Moran et al., 2024a, b).**

411 **3.7 Exceedances**

412 Widespread but low exceedances of acidity ($< 50 \text{ eq ha}^{-1} \text{ yr}^{-1}$) under average 2014–2016 deposition were found in
 413 regions in central and southern Quebec, Ontario, Manitoba, Alberta, British Columbia as well as in some regions in
 414 Nova Scotia and Newfoundland, under both protection levels (Figure 11). Further, exceedances above $200 \text{ eq ha}^{-1} \text{ yr}^{-1}$
 415 were predicted in southern Quebec and Ontario, as well as near Winnipeg and Vancouver, under both protection
 416 levels. Exceedances of acidity under 2014–2016 S and N deposition were not generally predicted in the north. The
 417 spatial extent of exceedance was slightly greater under the 5% protection limit as a result of lower $CL_{max}S$ and $CL_{max}N$,
 418 particularly around point sources of S and N, such as the AOSR.

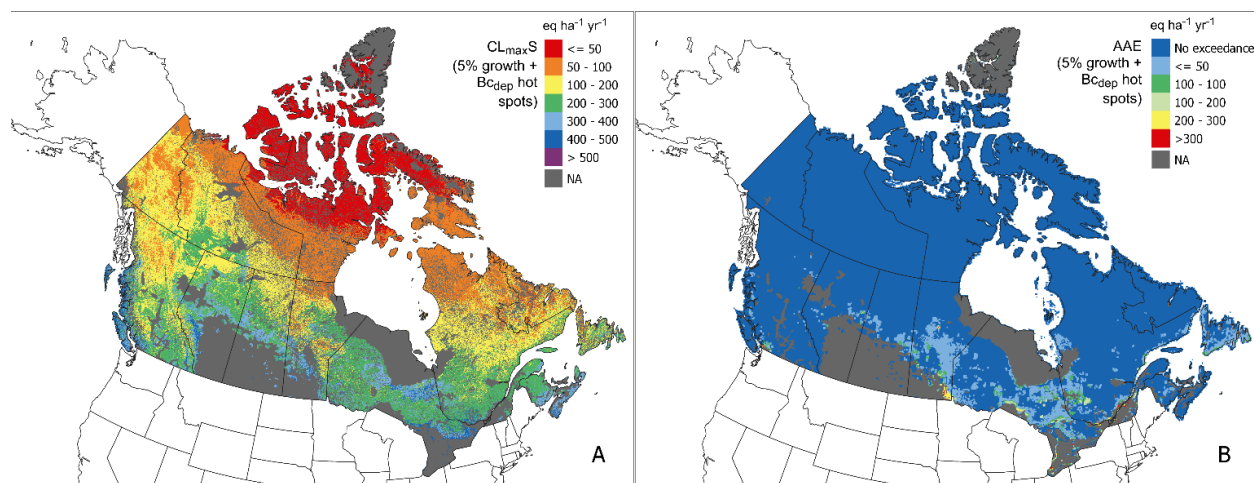
419
 420 If the Bc_{dep} without smoothing is employed (i.e., the base cation deposition associated with high magnitude
 421 anthropogenic sources is included), exceedances are reduced (see Figure 12B and compare to Figure 11B). The $CL_{max}S$
 422 based on anthropogenic-inclusive Bc_{dep} (at 5% protection level, Figure 12A) indicated that $CL_{max}S$ is elevated in the
 423 AOSR in comparison with the smoothed $CL_{max}S$ in Figure 8B.

424



425

426 **Figure 11: Average Accumulated Exceedance (AAE) of critical loads of acidity under 2014–2016 sulphur and nitrogen**
 427 **GEM-MACH modelled deposition. Two growth reduction scenarios are presented: using a chemical criterion representing**
 428 **20% growth reduction (A) and 5% growth reduction (B).**



429
 430 **Figure 12: A scenario using base cation deposition without smoothing, illustrating the impact of hot-spot BC_{dep} on the**
 431 **maximum critical load of sulphur (CL_{maxS}) (A) and the Average Accumulated Exceedance (AAE) under average 2014–2016**
 432 **sulphur and nitrogen GEM-MACH modelled deposition (B).**

433 Widespread exceedances of CL_{nutN} were predicted across most provinces, with generally low AAE ($< 50 \text{ eq ha}^{-1} \text{ yr}^{-1}$)
 434 extending to just north of 60° latitude, and higher values of $100\text{--}200 \text{ eq ha}^{-1} \text{ yr}^{-1}$ were predicted from Alberta east to
 435 Quebec (Figure 9B). Some regions adjacent to the agricultural ecumene in the Prairies, southern Ontario, Quebec and
 436 the AOSR experienced values above $300 \text{ eq ha}^{-1} \text{ yr}^{-1}$ up to $1053 \text{ eq ha}^{-1} \text{ yr}^{-1}$; however, 80% of grid cells in exceedance
 437 fell below $300 \text{ eq ha}^{-1} \text{ yr}^{-1}$.

438
 439 There were 12,341 sites of interest across Canada (i.e., PA and OECM areas); however, only 8,372 fall within areas
 440 assessed in this study (e.g. not within the agricultural ecumene or Hudson Bay Plains ecozone). In total, 10% of these
 441 sites exceeded CL_{maxS} under the 5% protection limit (Table 5). This was roughly double the number of sites in
 442 exceedance under the 20% protection limit. By comparison the BC_{dep} layer with unsmoothed hot spots (i.e. retaining
 443 higher BC_{dep} close to anthropogenic emissions areas) under the 5% protection limit showed a reduction in total areas
 444 that are in exceedance of acidity critical loads; anthropogenic emissions of base cations reduce the exceedances by
 445 increasing N_{up} values. The number of PA and OECM sites in exceedance of CL_{nutN} was much higher, 70% of total
 446 sites assessed (Table 5).

447
 448 **Table 5: Exceedance summarized by number of Protected Areas (PA) and Other Effective area-based Conservation**
 449 **Measures (OECM) areas (ECCC, 2023b) experiencing any exceedance. Three exceedance scenarios are presented: Critical**
 450 **load of acidity exceedance at 5% and 20% growth reduction protection levels, unsmoothed base cation deposition under**
 451 **the 5% scenario, and exceedance of nutrient nitrogen (CL_{nutN}). Critical loads of acidity and nutrient nitrogen were assessed**
 452 **under a multi-year (2014–2016) average GEM-MACH modelled sulphur and nitrogen total deposition.**

	PA	OECM	% Exceeded
Number of sites	8,205	167	-
Exceeded (5% growth reduction)	793	17	9.7

Exceeded (20% growth reduction)	313	10	3.9
Exceeded (5% with hot spots)	445	14	5.5
Exceeded ($CL_{nut}N$)	5,807	85	70.4

453

454 **4 Discussion**

455 **4.1 Uncertainties in critical loads of acidity and nutrient nitrogen**

456 Critical loads of acidity reflect the influence of BC_{we} , particularly in the north where cold annual temperatures slow
457 weathering rates to almost zero. However, areas near the Canada-U.S. border also showed lower BC_{we} rates by 200–
458 300 eq ha⁻¹ yr⁻¹ when corrected for temperature (Figure 4). Soil depth remains a poorly mapped parameter that has
459 significant impact on BC_{we} , and it is worth noting that average estimates were based on mapped soil depths (Hengl,
460 2017), which ranged from 1 cm to a maximum rooting depth of 30 or 50 cm. While comparison between mapped
461 values and site-level values is difficult (due to methodological differences and spatial representation), there are some
462 studies which have observational values in representative areas; for example, in northern Saskatchewan, 50% of 107
463 sites were estimated below 300 eq ha⁻¹ yr⁻¹, slightly above our mapped estimates of 230 eq ha⁻¹ yr⁻¹ for (primarily
464 northern) Saskatchewan (Table 4; Figure 4). Estimates for conifer stands in Québec by Ouimet et al. (2001) were 210
465 eq ha⁻¹ yr⁻¹, comparable to the mean 229 eq ha⁻¹ yr⁻¹ estimated for the Boreal Shield ecozone in our study (Table 4).
466 In British Columbia, Mongeon et al. (2010) found BC_{we} to be 710 eq ha⁻¹ yr⁻¹, much greater than the 235 eq ha⁻¹ yr⁻¹
467 estimated in our study for the Pacific Maritime ecozone. Koseva et al., (2010) estimated BC_{we} at 10 sites in Ontario
468 primarily in the Mixedwood Plains ecozone at 628 eq ha⁻¹ yr⁻¹ (compared to 306 eq ha⁻¹ yr⁻¹ over the Mixedwood
469 Plains in our study). Moreover, Koseva et al. suggest that the soil-texture approximation method (as used in our study)
470 under-estimates BC_{we} in comparison to the better-performing PROFILE model. Assessments of uncertainty in critical
471 load estimates recognize BC_{we} as the primary driver of uncertainty (Li and McNulty, 2007; Skeffington et al., 2006)
472 and, as such, observational data and PROFILE-modelled site data to constrain weathering rates would greatly improve
473 critical load estimates.

474

475 While the inclusion of a modelled BC_{dep} map represents an improvement over previous Canadian critical load projects,
476 several factors likely contribute to the BC_{dep} modelled negative bias (which has appeared in other publications, such
477 as Makar et al., 2018) and may relate to how emissions processing has been carried out for air-quality models in North
478 America. While anthropogenic emissions inventories include estimates of PM_{2.5}, PM₁₀ and PM_{total} mass emissions,
479 usually only PM_{2.5} and PM₁₀ emissions are used in determination of model input emissions. However, substantial
480 emitted base cation mass may reside in the larger size fractions (between the mass included within PM₁₀ and the
481 PM_{total}). The model version and emissions inventory data used in the base cation deposition estimates of AQMEII4
482 included only emissions up to 10 µm diameter, as did work examining emissions from multiple sources of primary
483 particulate matter (Boutzis et al., 2020). Subsequent work using observations from the Canadian Oil Sands and
484 reviewing other sources of data after Boutzis et al. (2020) and Galmarini et al. (2021) suggest that many of the same
485 sources of anthropogenic particulate matter emissions include emitted particles between 10 and 40 µm diameter, the
486 mass of which adds an additional 66% relative to the PM_{2.5} to PM₁₀ “coarse mode” emitted mass. For forest fire

487 emissions, this additional mass is much larger. The wildfire particulate matter size distributions of Radke et al. (1988;
488 1990) used to estimate mass up to PM_{10} in Boutzis et al. (2020) show that the emitted particle mass between 10 and
489 40 μm diameter is 7.26 times that emitted between $PM_{2.5}$ and PM_{10} . Approximately 9.7% of this particle mass is
490 composed of base cations (e.g., Table S5 of Chen et al., 2019). A third factor is another natural emissions source,
491 aeolian or wind-blown dust emissions (e.g., Bullard et al., 2016; Park et al., 2010), which was not included in the
492 AQMEII4 simulations. These (traditionally missing) sources of base cation mass in air-quality models likely
493 contribute to the substantial negative bias noted here. Nevertheless, regression in Figure 3 suggests that the spatial
494 distribution of base cations emissions and deposition from Galmarini et al. (2021) is reasonable, and we have used the
495 relationship between modelled and observed values to provide corrected estimates of Bc_{dep} .

496
497 The conservative 5% protection level set for the Bc/Al_{crit} is favoured by the authors of the current work for critical
498 loads estimates, which affords greater ecosystem protection consistent with studies using $Bc/Al > 1$ (e.g. McDonnell
499 et al., 2023; Mongeon et al., 2010; Ouimet et al., 2006). Historically, when acidic deposition was higher than at
500 present, a 20% growth reduction was a reasonable target. However, under decreasing emissions and deposition, as
501 well as acceptable impacts to wood production, carbon storage, and ecosystem health there is greater certainty in
502 ecosystem protection under the 5% protection level. It should be noted that the level of protection is a policy decision
503 regarding how much should be protected, rather than a sensitivity, and taking the most sensitive species through the
504 Bc/Al_{crit} selection process ensures the highest possible protection based on species-specific dose-response curves.
505 Note, however, that changes to forest health and climate may also induce pressures that are not captured in the selection
506 of the Bc/Al_{crit} from the studies described in Sverdrup & Warfvinge (1993).

507
508 $CL_{nut}N$ seems to be driven primarily by Q rather than by vegetation cover; low $CL_{nut}N$ was seen in regions of
509 correspondingly low Q values (e.g., $>50 \text{ mm yr}^{-1}$) in much of the Arctic and central Canada. In contrast, areas with
510 high Q were found to result in high $CL_{nut}N$; as previously suggested by Reinds et al. (2015), a critical flux rather than
511 concentration may provide more reliable critical loads in regions with elevated precipitation such as the Pacific
512 Maritime ecozone in British Columbia.

513
514 The omission of wetlands, which cover an estimated 13% of land in Canada, from acidity and nutrient N critical loads
515 represents a gap in terrestrial (and aquatic) ecosystem protection. Although there are modifications to the SMB model
516 that address critical loads for wetlands, this study was limited by the availability of a suitable national wetlands
517 classification map. Future studies may address this data gap as wetland classification products become available.

518 **4.2 Exceedances of critical loads**

519 Historically, forests in eastern Canada were regarded as ecosystems most susceptible to acidification due to their
520 underlying geology, shallow soil type, vegetation, and elevated acidic deposition from domestic and transboundary
521 air pollution. This study adds to the body of literature supporting recent studies in both terrestrial and aquatic critical
522 loads (e.g., Makar et al., 2018; Cathcart et al., 2016; Williston et al., 2016; Mongeon et al., 2010; Whitfield et al.,

2010), showing likely exceedance of critical loads of acidity in central and western Canada (i.e., in regions such as Alberta, Saskatchewan and British Columbia). The prevalence of our predicted widespread exceedances in Manitoba (Figure 10) may reflect low mineral soil depth, as organic soil dominates this part of the country. Further, point sources (generally large mining or smelting operations) remain a concern (e.g., in southern Manitoba, the AOSR, and southern British Columbia) with regard to sharply elevated local exceedance, which may be temporally mitigated by elevated BC_{dep} from co-located dust emissions sources. Additionally, high BC_{dep} can have an alkalizing impact on ecosystems. In China, where elevated BC_{dep} emissions from industrialization have historically mitigated the effects of acidic deposition in many regions, successful particle emissions mitigation strategies have reduced BC_{dep} in recent years (as S and N deposition have declined), resulting in increased critical load exceedance (Zhao et al., 2021). However, the steady-state assumptions of the SMB require non-anthropogenic BC_{dep} , since they must reflect long-term conditions, and base cation emissions cannot be reliably coupled with changes to those of S and N and should be considered separately.

Widespread $CL_{nut}N$ exceedance (found in the majority of the PA and OECM sites assessed) suggests that nutrient N may present a risk to biodiversity at many sites under protective measures. However, 40% of the grid cells showing $CL_{nut}N$ exceedance were below $50 \text{ eq ha}^{-1} \text{ yr}^{-1}$ and it is likely that many of these exceedances are within the uncertainty of the model. While some empirical studies of nutrient N have been done in Canada, a large knowledge gap exists for many Canadian ecosystems regarding the effect of nutrient nitrogen and their critical loads. Some work has developed on Jack pine and northern ecosystems; Vandinther suggested that across Jack pine-dominant forests surrounding the AOSR, the biodiversity-based empirical critical load of nutrient N was $5.6 \text{ kg ha}^{-1} \text{ yr}^{-1}$ ($400 \text{ eq ha}^{-1} \text{ yr}^{-1}$; Vandinther and Aherne, 2023a) which is above the maximum $CL_{nut}N$ calculated in this study within 200 km of the AOSR ($216 \text{ eq ha}^{-1} \text{ yr}^{-1}$). Further, in low deposition ‘background’ regions a biodiversity-based empirical critical load of $1.4 - 3.15 \text{ kg ha}^{-1} \text{ yr}^{-1}$ ($100 - 225 \text{ eq ha}^{-1} \text{ yr}^{-1}$) was found to protect lichen communities and other N-sensitive species in Jack pine forests across Northwestern Canada (Vandinther and Aherne, 2023b); these are again higher compared to mean values in this study (e.g. for the Boreal Plain, $76 \text{ eq ha}^{-1} \text{ yr}^{-1}$). Empirical critical loads developed for ecoregions in Northern Saskatchewan (Murray et al., 2017) fall into a range of $88 - 123 \text{ eq ha}^{-1} \text{ yr}^{-1}$, again higher than values suggested by this study (e.g. $62 \text{ eq ha}^{-1} \text{ yr}^{-1}$ in Saskatchewan). In comparison to these empirical values, $CL_{nut}N$ values in the current work are lower by a factor of 2. If $CL_{nut}N$ is doubled, only 10% of the soils assessed are in exceedance (versus 31% of soils). This reduction in the areal exceedance would in turn reduce the number of PA and OECM sites in exceedance. While the spatial pattern of $CL_{nut}N$ exceedances does not generally follow exceedances of critical loads of acidity, some areas (including PA and OECM sites) in central Canada were estimated to be in exceedance of both critical loads of acidity and nutrient N, suggesting that this region may be of particular concern. Given the largest areal exceedance is of $CL_{nut}N$, observational studies with the view of expanding Canadian ecosystem empirical critical loads would help determine how, and by how much, Canadian ecosystems are affected by N_{dep} and how well these observations align with $CL_{nut}N$ in the current work. Additionally, vegetation community changepoint modelling such with the TITAN model (Baker, 2010) could help bring understanding to how Canadian ecosystems might experience elevated N_{dep} with regard to changes in biodiversity.

560 **5 Conclusions**

561 This study mapped critical loads of acidity and nutrient nitrogen for terrestrial ecosystems the using the steady-state
562 SMB model. The modelling approach used (a) high-resolution national maps of soils, meteorology, and forest
563 composition, (b) high-resolution modelled Canada-wide BC_{dep} , and (c) species-specific chemical criteria for damage.
564 The resulting national critical loads of acidity and nutrient N for Canadian terrestrial ecosystems were mapped at a
565 250 m resolution. The influence of different levels of protection and BC_{dep} models was also explored, including two
566 vegetation protection levels (5% and 20% root biomass growth reduction scenarios) and anthropogenic base cation
567 deposition “hot spots”.

568
569 Terrestrial ecosystems in Canada continue to receive acidic deposition in excess of their critical loads for both acidity
570 and nutrient N under modelled (2014–2016 average) total S and N deposition in areas of both eastern and western
571 Canada. These areas include several major point emissions sources including the Alberta Oil Sands Region. Further,
572 exceedance was predicted at 10% (acidity) and 70% (nutrient nitrogen) of the assessed sites (PA and OECM) where
573 preserving biodiversity is a national policy goal, suggesting that current levels of N deposition may be affecting a
574 large majority of these ecologically important sites. Soil recovery from acidic deposition is a slow process that may
575 take decades or even centuries to reach pre-acidification levels, which cannot begin until deposition falls below critical
576 loads. Parameterization of the SMB model specifically for Canadian ecosystems is a step forward in refining Canadian
577 terrestrial critical loads, and the maps produced by this study are a valuable tool in identifying and assessing regions
578 sensitive to acidic deposition and nutrient N deposition, as well as providing a foundation for more refined provincial
579 estimates.

580 **CRedit authorship contribution statement**

581 **H. Cathcart:** Conceptualization, Data curation, Investigation, Methodology, Formal analysis, Visualization, Writing
582 – original draft, Writing – review & editing. **J. Aherne:** Formal analysis, Methodology, Writing – review &
583 editing. **M.D. Moran:** Data curation, Investigation, Methodology, Writing – original draft, Writing – review &
584 editing. **V. Savic-Jovicic:** Data curation, Investigation. **P.A. Makar:** Investigation, Methodology, Writing – original
585 draft, Writing – review & editing. **A.D Cole:** Writing – review & editing.

586 **Competing interests**

587 The authors declare that they have no conflict of interest.

588 **Data availability**

589 Raster files of critical load maps (CL_{maxS} , CL_{maxN} , CL_{minN} , CL_{nutN}) will be made available on the Government of
590 Canada’s Open Data Portal under Environment and Climate Change Canada’s records
591 (<https://open.canada.ca/data/organization/ec>) at <https://doi.org/10.18164/ec5c8bbb-3bc8-4675-a9c6-103add874b8>.

592 **Acknowledgements**

593 This study was funded by Environment and Climate Change Canada. The authors wish to acknowledge Max Posch
594 for his provision of (and guidance regarding) soil water runoff (Q) estimates, and the AQMEII4 project for emissions
595 data leading to GEM-MACH maps of base cation deposition.

596 **Copyright**

597 The works published in this journal are distributed under the Creative Commons Attribution 4.0 License. This licence
598 does not affect the Crown copyright work.

599
600 © His Majesty the King in Right of Canada, as represented by the Minister of Environment and Climate Change
601 Canada, 2024.

602 **References**

603 Agriculture and Agri-Food Canada: Terrestrial Ecozones of Canada [dataset], [https://open.canada.ca/data/en/dataset/7ad7ea01-](https://open.canada.ca/data/en/dataset/7ad7ea01-eb23-4824-bccc-66adb7c5bdf8)
604 [eb23-4824-bccc-66adb7c5bdf8](https://open.canada.ca/data/en/dataset/7ad7ea01-eb23-4824-bccc-66adb7c5bdf8), 2013.

605 Aherne, J. and Posch, M.: Impacts of nitrogen and sulphur deposition on forest ecosystem services in Canada, *Curr. Opin.*
606 *Environ. Sustain.*, 5, 108–115, <https://doi.org/10.1016/j.cosust.2013.02.005>, 2013.

607 Aklilu, Y.-A., Blair, L., Dinwoodie, G., and Aherne, J.: Using steady-state mass balance model to determine critical loads of
608 acidity for terrestrial ecosystems in Alberta, Government of Alberta, Ministry of Environment and Parks, 2022.

609 Baker, M. E. and King, R. S.: A new method for detecting and interpreting biodiversity and ecological community thresholds,
610 *Methods Ecol. Evol.*, 1, 25–37, <https://doi.org/10.1111/j.2041-210X.2009.00007.x>, 2010.

611 Beaudoin, A., Bernier, P. Y., Guindon, L., Villemare, P., Guo, X. J., Stinson, G., Bergeron, T., Magnussen, S., and Hall, R. J.:
612 Mapping attributes of Canada’s forests at moderate resolution through kNN and MODIS imagery, *Can. J. For. Res.*, 44, 521–532,
613 <https://doi.org/10.1139/cjfr-2013-0401>, 2014.

614 Bobbink, R. and Hicks, W. K.: Factors Affecting Nitrogen Deposition Impacts on Biodiversity: An Overview, in: Nitrogen
615 Deposition, Critical Loads and Biodiversity, edited by: Sutton, M. A., Mason, K. E., Sheppard, L. J., Sverdrup, H., Haeuber, R.,
616 and Hicks, W. K., Springer Netherlands, Dordrecht, 127–138, https://doi.org/10.1007/978-94-007-7939-6_14, 2014.

617 Bobbink, R., Loran, C., and Tomassen, H.: Review and revision of empirical critical loads of nitrogen for Europe,
618 Umweltbundesamt/German Environment Agency, Dessau-Roßlau, Germany, 2022.

619 Bonten, L. T. C., Reinds, G. J., and Posch, M.: A model to calculate effects of atmospheric deposition on soil acidification,
620 eutrophication and carbon sequestration, *Environ. Model. Softw.*, 79, 75–84, <https://doi.org/10.1016/j.envsoft.2016.01.009>, 2016.

621 Boutzis, E. I., Zhang, J., and Moran, M. D.: Expansion of a size disaggregation profile library for particulate matter emissions
622 processing from three generic profiles to 36 source-type-specific profiles, *J. Air Waste Manag. Assoc.*, 70, 1067–1100,
623 <https://doi.org/10.1080/10962247.2020.1743794>, 2020.

624 Bouwman, A. F., Vuuren, D. P. V., Derwent, R. G., and Posch, M.: A Global Analysis of Acidification and Eutrophication of
625 Terrestrial Ecosystems, *Water. Air. Soil Pollut.*, 141, 349–382, <https://doi.org/10.1023/A:1021398008726>, 2002.

626 Bullard, J. E., Baddock, M., Bradwell, T., Crusius, J., Darlington, E., Gaiero, D., Gassó, S., Gisladdottir, G., Hodgkins, R.,
627 McCulloch, R., McKenna-Neuman, C., Mockford, T., Stewart, H., and Thorsteinsson, T.: High-latitude dust in the Earth system,
628 *Rev. Geophys.*, 54, 447–485, <https://doi.org/10.1002/2016RG000518>, 2016.

629 Burns, D. A., Blett, T., Haeuber, R., and Pardo, L. H.: Critical loads as a policy tool for protecting ecosystems from the effects of
630 air pollutants, *Front. Ecol. Environ.*, 6, 156–159, <https://doi.org/10.1890/070040>, 2008.

631 Carou, S., Dennis, I., Aherne, J., Ouimet, R., Arp, P. A., Watmough, S. A., DeMerchant, I., Shaw, M., Vet, B., Bouchet, V., and
632 Moran, M.: A national picture of acid deposition critical loads for forest soils in Canada, Canadian Council of Ministers of the
633 Environment, Winnipeg, Manitoba, 2008.

634 Cathcart, H., Aherne, J., Jeffries, D. S., and Scott, K. A.: Critical loads of acidity for 90,000 lakes in northern Saskatchewan: A
635 novel approach for mapping regional sensitivity to acidic deposition, *Atmos. Environ.*, 146, 290–299,
636 <https://doi.org/10.1016/j.atmosenv.2016.08.048>, 2016.

637 CEC: 2010 Land Cover of North America at 250 meters (v2.0) [dataset], Commission for Environmental Cooperation (CEC).
638 Canada Centre for Remote Sensing (CCRS), U.S. Geological Survey (USGS), Comisión Nacional para el Conocimiento y Uso de
639 la Biodiversidad (CONABIO), Comisión Nacional Forestal (CONAFOR), Instituto Nacional de Estadística y Geografía (INEGI),
640 <http://www.cec.org/north-american-environmental-atlas/land-cover-2010-modis-250m>, 2018.

641 Chen, J., Anderson, K., Pavlovic, R., Moran, M. D., Englefield, P., Thompson, D. K., Munoz-Alpizar, R., and Landry, H.: The
642 FireWork v2.0 air quality forecast system with biomass burning emissions from the Canadian Forest Fire Emissions Prediction
643 System v2.03, *Geosci. Model Dev.*, 12, 3283–3310, <https://doi.org/10.5194/gmd-12-3283-2019>, 2019.

644 Clark, C. M., Morefield, P. E., Gilliam, F. S., and Pardo, L. H.: Estimated losses of plant biodiversity in the United States from
645 historical N deposition (1985–2010), *Ecology*, 94, 1441–1448, <https://doi.org/10.1890/12-2016.1>, 2013.

646 CLBBR: Soil Landscapes of Canada, v. 2.2 [dataset], Centre for Land and Biological Resources Research. Research Branch,
647 Agriculture and Agri-Food Canada, <https://sis.agr.gc.ca/cansis/nsdb/slc/v2.2>, 1996.

648 CLRTAP: Mapping critical loads for ecosystems, Chapter V of Manual on methodologies and criteria for modelling and mapping
649 critical loads and levels and air pollution effects, risks and trends. UNECE Convention on Long-range Transboundary Air
650 Pollution, at www.icpmapping.org, 2015.

651 Cronan, C. S. and Schofield, C. L.: Relationships between aqueous aluminum and acidic deposition in forested watersheds of
652 North America and northern Europe, *Environ. Sci. Technol.*, 24, 1100–1105, <https://doi.org/10.1021/es00077a022>, 1990.

653 De Vries, W., Posch, M., Reinds, G. J., and Kämäri, J.: Critical loads and their exceedance on forest soils in Europe, Report - The
654 Winand Staring Centre for Integrated Land, Soil and Water Research (SC_DLO), Wageningen, the Netherlands, 123 pp., 1992.

655 De Vries, W., Hettelingh, J.-P., and Posch, M. (Eds.): The History and Current State of Critical Loads and Dynamic Modelling
656 Assessments, in: Critical loads and dynamic risk assessments: Nitrogen, acidity and metals in terrestrial and aquatic ecosystems,
657 Springer, 1–11, https://doi.org/10.1007/978-94-017-9508-1_1, 2015.

658 Dymond, C. C., Titus, B. D., Stinson, G., and Kurz, W. A.: Future quantities and spatial distribution of harvesting residue and
659 dead wood from natural disturbances in Canada, *For. Ecol. Manag.*, 260, 181–192, <https://doi.org/10.1016/j.foreco.2010.04.015>,
660 2010.

661 ECCC: Evaluation of the Addressing Air Pollution Horizontal Initiative, Environment and Climate Change Canada, ISBN: 978-
662 0-660-39645-3, 2021.

663 ECCC: Canadian Environmental Sustainability Indicators: Extent of Canada’s Wetlands, ISBN: 978-0-660-05390-5, 2016.

664 ECCC: 2022 Canadian Protected and Conserved Areas Database (CPCAD) User Manual, Environment and Climate Change
665 Canada, [https://data-donnees.ec.gc.ca/data/species/protectstore/canadian-protected-conserved-areas-
666 database/ProtectedConservedAreaUserManual.pdf](https://data-donnees.ec.gc.ca/data/species/protectstore/canadian-protected-conserved-areas-database/ProtectedConservedAreaUserManual.pdf), 2023a.

667 ECCC: Canadian Protected and Conserved Areas Database 2022 [dataset], Environment and Climate Change Canada,
668 <https://www.canada.ca/en/environment-climate-change/services/national-wildlife-areas/protected-conserved-areas-database.html>,
669 2023b.

670 ECCC: Toward a 2030 Biodiversity Strategy for Canada: Halting and Reversing Nature Loss, Environment and Climate Change
671 Canada, ISBN: 978-0-660-48594-2, 2023c.

672 ECCC: Canada's air pollutant emissions inventory report 1990-2022., Environment and Climate Change Canada. ISSN: 2562-
673 4903. https://publications.gc.ca/collections/collection_2024/eccc/En81-30-2022-eng.pdf, Gatineau, Quebec, 2024.

674 FAO-UNESCO: Digital soil map of the world and derived soil properties, CD-ROM, Rome, ISBN: 978-92-3-103889-1, 92-3-
675 103889-3, 2003.

676 Feng, J., Vet, R., Cole, A., Zhang, L., Cheng, I., O'Brien, J., and Macdonald, A.-M.: Inorganic chemical components in
677 precipitation in the eastern U.S. and Eastern Canada during 1989–2016: Temporal and regional trends of wet concentration and
678 wet deposition from the NADP and CAPMoN measurements, *Atmos. Environ.*, 254, 118367,
679 <https://doi.org/10.1016/j.atmosenv.2021.118367>, 2021.

680 Forsius, M., Posch, M., Aherne, J., Reinds, G., Christensen, J., and Hole, L.: Assessing the Impacts of Long-Range Sulfur and
681 Nitrogen Deposition on Arctic and Sub-Arctic Ecosystems, *Ambio*, 39, 136–47, <https://doi.org/10.1007/s13280-010-0022-7>,
682 2010.

683 Galmarini, S., Makar, P., Clifton, O. E., Hogrefe, C., Bash, J. O., Bellasio, R., Bianconi, R., Bieser, J., Butler, T., Ducker, J.,
684 Flemming, J., Hodzic, A., Holmes, C. D., Kioutsioukis, I., Kranenburg, R., Lupascu, A., Perez-Camanyo, J. L., Pleim, J., Ryu,
685 Y.-H., San Jose, R., Schwede, D., Silva, S., and Wolke, R.: Technical note: AQMEII4 Activity 1: evaluation of wet and dry
686 deposition schemes as an integral part of regional-scale air quality models, *Atmospheric Chem. Phys.*, 21, 15663–15697,
687 <https://doi.org/10.5194/acp-21-15663-2021>, 2021.

688 Hazlett, P., Emilson, C., Lawrence, G., Fernandez, I., Ouimet, R., and Bailey, S.: Reversal of Forest Soil Acidification in the
689 Northeastern United States and Eastern Canada: Site and Soil Factors Contributing to Recovery, *Soil Syst.*, 4, 54,
690 <https://doi.org/10.3390/soilsystems4030054>, 2020.

691 Hengl, T.: SoilGrids250m 2017-03 Absolute depth to bedrock (in cm). [dataset], ISRIC - World Soil Inf.,
692 <https://data.isric.org/geonetwerk/srv/api/records/f36117ea-9be5-4afd-bb7d-7a3e77bf392a>, 2017.

693 Hengl, T.: Clay content in % (kg / kg) at 6 standard depths (0, 10, 30, 60, 100 and 200 cm) at 250 m resolution (v0.2). [dataset],
694 Zenodo, <https://doi.org/10.5281/zenodo.2525663>, 2018a.

695 Hengl, T.: Coarse fragments % (volumetric) at 6 standard depths (0, 10, 30, 60, 100 and 200 cm) at 250 m resolution [dataset],
696 <https://doi.org/10.5281/zenodo.2525682>, 2018b.

697 Hengl, T.: Sand content in % (kg / kg) at 6 standard depths (0, 10, 30, 60, 100 and 200 cm) at 250 m resolution (v0.2) [dataset],
698 Zenodo, <https://doi.org/10.5281/zenodo.2525662>, 2018c.

699 Hengl, T.: Soil bulk density (fine earth) 10 x kg / m-cubic at 6 standard depths (0, 10, 30, 60, 100 and 200 cm) at 250 m
700 resolution (v0.2) [dataset], Zenodo, <https://doi.org/10.5281/zenodo.2525665>, 2018d.

701 Hengl, T. and Wheeler, I.: Soil organic carbon content in x 5 g / kg at 6 standard depths (0, 10, 30, 60, 100 and 200 cm) at 250 m
702 resolution (v0.2) [dataset], Zenodo, <https://doi.org/10.5281/zenodo.2525553>, 2018.

703 Hijmans, R.J.: terra: Spatial Data Analysis. R package version 1.7-23, <https://CRAN.R-project.org/package=terra,2023>.

704 Johnson, Dale W., and John Turner: Nitrogen budgets of forest ecosystems: a review, *Forest Ecology and Management* 318,370-
705 379, <https://doi.org/10.1016/j.foreco.2013.08.028>, 2014.

706 Koseva, I. S., Watmough, S. A., and Aherne, J.: Estimating base cation weathering rates in Canadian forest soils using a simple
707 texture-based model, *Biogeochemistry*, 101, 183–196, <https://doi.org/10.1007/s10533-010-9506-6>, 2010.

708 Lawrence, G. B., David, M. B., Lovett, G. M., Murdoch, P. S., Burns, D. A., Stoddard, J. L., Baldigo, B. P., Porter, J. H., and
709 Thompson, A. W.: Soil Calcium Status and the Response of Stream Chemistry to Changing Acidic Deposition Rates, *Ecol.*
710 *Appl.*, 9, 1059–1072, [https://doi.org/10.1890/1051-0761\(1999\)009\[1059:SCSATR\]2.0.CO;2](https://doi.org/10.1890/1051-0761(1999)009[1059:SCSATR]2.0.CO;2), 1999.

711 Lawrence, G. B., Hazlett, P. W., Fernandez, I. J., Ouimet, R., Bailey, S. W., Shortle, W. C., Smith, K. T., and Antidormi, M. R.:
712 Declining Acidic Deposition Begins Reversal of Forest-Soil Acidification in the Northeastern U.S. and Eastern Canada, *Environ.*
713 *Sci. Technol.*, 49, 13103–13111, <https://doi.org/10.1021/acs.est.5b02904>, 2015.

- 714 Li, H. and McNulty, S. G.: Uncertainty analysis on simple mass balance model to calculate critical loads for soil acidity, *Environ. Pollut.*, 149, 315–26, <https://doi.org/10.1016/j.envpol.2007.05.014>, 2007.
- 715
- 716 Liang, T. and Aherne, J.: Critical loads of acidity and exceedances for 1138 lakes and ponds in the Canadian Arctic, *Sci. Total Environ.*, 652, 1424–1434, <https://doi.org/10.1016/j.scitotenv.2018.10.330>, 2019.
- 717
- 718 Likens, G. E., Driscoll, C. T., and Buso, D. C.: Long-term effects of acid rain: response and recovery of a forest ecosystem, *Science*, 272, 244–246, <https://doi.org/10.1126/science.272.5259.244>, 1996.
- 719
- 720 Makar, P. A., Akingunola, A., Aherne, J., Cole, A. S., Aklilu, Y., Zhang, J., Wong, I., Hayden, K., Li, S.-M., Kirk, J., Scott, K.,
721 Moran, M. D., Robichaud, A., Cathcart, H., Baratzedah, P., Pabla, B., Cheung, P., Zheng, Q., and Jeffries, D. S.: Estimates of
722 exceedances of critical loads for acidifying deposition in Alberta and Saskatchewan, *Atmospheric Chem. Phys.*, 18, 9897–9927,
723 <https://doi.org/10.5194/acp-18-9897-2018>, 2018.
- 724 Mandre, M., Kask, R., Pikk, J., and Ots, K.: Assessment of growth and stemwood quality of Scots pine on territory influenced by
725 alkaline industrial dust, *Environ. Monit. Assess.*, 138, 51–63, <https://doi.org/10.1007/s10661-007-9790-3>, 2008.
- 726 McDonnell, T. C., Phelan, J., Talhelm, A. F., Cosby, B. J., Driscoll, C. T., Sullivan, T. J., and Greaver, T.: Protection of forest
727 ecosystems in the eastern United States from elevated atmospheric deposition of sulfur and nitrogen: A comparison of steady-
728 state and dynamic model results, *Environ. Pollut.*, 318, 120887, <https://doi.org/10.1016/j.envpol.2022.120887>, 2023.
- 729 McKenney, D., Papadopol, P., Campbell, K., Lawrence, K., Hutchinson, M., and others: Spatial models of Canada-and North
730 America-wide 1971/2000 minimum and maximum temperature, total precipitation and derived bioclimatic variables. *Frontline*
731 *Technical Note* 106., 2006.
- 732 Mongeon, A., Aherne, J., and Watmough, S. A.: Steady-state critical loads of acidity for forest soils in the Georgia Basin, *British*
733 *Columbia, J. Limnol.*, 69, 193–200, <https://doi.org/10.4081/jlimnol.2010.s1.193>, 2010.
- 734 Moran, M. D., Savic-Jovcic, V., Makar, P. A., Gong, W., Stroud, C. A., Zhang, J., Zheng, Q., Chen, J., Akingunola, A., Lupu, A.,
735 Ménard, S., Menelaou, K., and Munoz-Alpizar, R.: Operational chemical weather forecasting with the ECCC online Regional Air
736 Quality Deterministic Prediction System version 023 (RAQDPS023) - Part 1: System description, *Geosci Model Dev Prep.*,
737 2024a.
- 738 Moran, M. D., Lupu, A., Savic-Jovcic, V., Zhang, J., Zheng, Q., Boutzis, E., Mashayekhi, R., Stroud, C. A., Ménard, S., Chen, J.,
739 Menelaou, K., Munoz-Alpizar, R., Kornic, D., and Manseau, P.: Operational chemical weather forecasting with the ECCC online
740 Regional Air Quality Deterministic Prediction System version 023 (RAQDPS023) - Part 2: Prospective and retrospective
741 performance evaluations, *Geosci Model Dev Prep.*, 2024b.
- 742 Murray, C. A., Whitfield, C. J., and Watmough, S. A.: Uncertainty-based terrestrial critical loads of nutrient nitrogen in northern
743 Saskatchewan, Canada, *Boreal Environ. Res.*, 22(1-6), 2017.
- 744 Myers-Smith, I.H., Kerby, J.T., Phoenix, G.K. et al: Complexity revealed in the greening of the Arctic. *Nat. Clim. Chang.* 10,
745 106–117, <https://doi.org/10.1038/s41558-019-0688-1>, 2020.
- 746 NADP: National Trends Network [dataset], National Atmospheric Deposition Program (NRSP-3). NADP Program Office,
747 Wisconsin State Laboratory of Hygiene, 465 Henry Mall, Madison, WI 53706, <https://nadp.slh.wisc.edu/networks/national-trends-network>, 2023.
- 748
- 749 National Wetlands Working Group: The Canadian Wetland Classification System, 2nd ed, edited by: Warner, B.G., Rubec,
750 C.D.A., National Wetlands Working Group, Wetlands Research Branch, University of Waterloo, Waterloo, ON, Canada, 1997.
- 751 NEG-ECP: Critical Load of Sulphur and Nitrogen Assessment and Mapping Protocol for Upland Forests, N. Engl. Gov. East.
752 *Can. Prem. Environ. Task Group Acid Rain Action Plan Halifax N. S.*, 2001.
- 753 Nilsson, J. and Grenfelt, P.: Critical loads for sulphur and nitrogen, Nordic Council of Ministers, Copenhagen., Denmark, 1988.
- 754 Ouimet, R., Duchesne, L., Houle, D., and Arp, P.: Critical Loads and Exceedances of Acid Deposition and Associated Forest
755 Growth in the Northern Hardwood and Boreal Coniferous Forests in Québec, Canada, *Water Air Soil Pollut. Focus*, 1, 119–134,
756 <https://doi.org/10.1023/A:1011544325004>, 2001.

757 Ouimet, R., Arp, P. A., Watmough, S. A., Aherne, J., and DeMerchant, I.: Determination and Mapping Critical Loads of Acidity
758 and Exceedances for Upland Forest Soils in Eastern Canada, *Water, Air, Soil Pollut.*, 172, 57–66, [https://doi.org/10.1007/s11270-](https://doi.org/10.1007/s11270-005-9050-5)
759 005-9050-5, 2006.

760 Paal, J., Degtjarenko, P., Suija, A., and Liira, J.: Vegetation responses to long-term alkaline cement dust pollution in inus
761 sylvestris-dominated boreal forests – niche breadth along the soil pH gradient, *Appl. Veg. Sci.*, 16, 248–259,
762 <https://doi.org/10.1111/j.1654-109X.2012.01224.x>, 2013.

763 Pardo, L. H., Duarte, N., Miller, E. K., and Robin-Abbott, M.: Tree chemistry database (version 1.0), USDA For. Serv.
764 Northeast. Res. Stn., 324, <https://doi.org/10.2737/NE-GTR-324>, 2005.

765 Pardo, L. H., Coombs, J. A., Robin-Abbott, M. J., Pontius, J. H., and D'Amato, A. W.: Tree species at risk from nitrogen
766 deposition in the northeastern United States: A geospatial analysis of effects of multiple stressors using exceedance of critical
767 loads, *For. Ecol. Manag.*, 454, 117528, <https://doi.org/10.1016/j.foreco.2019.117528>, 2019.

768 Paré, D., Bernier, P., Lafleur, B., Titus, B. D., Thiffault, E., Maynard, D. G., and Guo, X.: Estimating stand-scale biomass,
769 nutrient contents, and associated uncertainties for tree species of Canadian forests, *Can. J. For. Res.*, 43, 599–608,
770 <https://doi.org/10.1139/cjfr-2012-0454>, 2013.

771 Park, S. H., Gong, S. L., Gong, W., Makar, P. A., Moran, M. D., Zhang, J., and Stroud, C. A.: Relative impact of windblown dust
772 versus anthropogenic fugitive dust in PM_{2.5} on air quality in North America, *J. Geophys. Res. Atmospheres*, 115,
773 <https://doi.org/10.1029/2009JD013144>, 2010.

774 Posch, M., de Smet, P. A. M., Hettelingh, J.-P., and Downing, R. J.: Calculation and Mapping of Critical Thresholds in Europe:
775 Status Report 1999, Coordination Center for Effects, National Institute of Public Health and the Environment, Bilthoven,
776 Netherlands, 1999.

777 Posch, M., de Vries, W., and Sverdrup, H. U.: Mass Balance Models to Derive Critical Loads of Nitrogen and Acidity for
778 Terrestrial and Aquatic Ecosystems, in: *Critical Loads and Dynamic Risk Assessments: Nitrogen, Acidity and Metals in*
779 *Terrestrial and Aquatic Ecosystems*, edited by: de Vries, W., Hettelingh, J.-P., and Posch, M., Springer Netherlands, Dordrecht,
780 171–205, https://doi.org/10.1007/978-94-017-9508-1_6, 2015.

781 Pribyl, D. W.: A critical review of the conventional SOC to SOM conversion factor, *Geoderma*, 156, 75–83,
782 <https://doi.org/10.1016/j.geoderma.2010.02.003>, 2010.

783 QGIS Development Team: QGIS Geographic Information System, Open Source Geospatial Foundation
784 Project, <http://qgis.osgeo.org>, 2023.

785 R Core Team: R: A Language and Environment for Statistical Computing, version 4.1.0, R Foundation for Statistical Computing,
786 Vienna, Austria, 2021.

787 Radke, L., Hegg, D., Lyons, J., Brock, C., Hobbs, P., Weiss, R., and Rasmussen, R.: Airborne measurements on smokes from
788 biomass burning, *Aerosols Clim.*, 411–422, 1988.

789 Radke, L. F., Lyons, J. H., Hobbs, P. V., Hegg, D. A., Sandberg, D. V., and Ward, D. E.: Airborne monitoring and smoke
790 characterization of prescribed fires on forest lands in western Washington and Oregon, US Department of Agriculture, Forest
791 Service, Pacific Northwest Research Station, 1990.

792 Reinds, G. J., Posch, M., Aherne, J., and Forsius, M.: Assessment of Critical Loads of Sulphur and Nitrogen and Their
793 Exceedances for Terrestrial Ecosystems in the Northern Hemisphere, in: *Critical loads and dynamic risk assessments: Nitrogen,*
794 *acidity and metals in terrestrial and aquatic ecosystems*, edited by: De Vries, W., Hettelingh, J.-P., and Posch, M., Springer, 403–
795 418, https://doi.org/10.1007/978-94-017-9508-1_15, 2015.

796 Reinds, G. J., Thomas, D., Posch, M., and Slotweg, J.: Critical loads for eutrophication and acidification for European terrestrial
797 ecosystems, Umweltbundesamt, Wörlitzer Platz 1, 06844 Dessau-Roßlau, Germany, 2021.

798 Rosen, K., Gundersen, P., Tegnhammar, L., Johansson, M., and Frogner, T.: Nitrogen enrichment of Nordic forest ecosystems:
799 the concept of critical loads, *Ambio*, 21:5, 364–368, 1992.

800 Shangguan, W., Hengl, T., Mendes de Jesus, J., Yuan, H., and Dai, Y.: Mapping the global depth to bedrock for land surface
801 modeling, *J. Adv. Model. Earth Syst.*, 9, 65–88, <https://doi.org/10.1002/2016MS000686>, 2017.

802 Simkin, S. M., Allen, E. B., Bowman, W. D., Clark, C. M., Belnap, J., Brooks, M. L., Cade, B. S., Collins, S. L., Geiser, L. H.,
803 Gilliam, F. S., Jovan, S. E., Pardo, L. H., Schulz, B. K., Stevens, C. J., Suding, K. N., Throop, H. L., and Waller, D. M.:
804 Conditional vulnerability of plant diversity to atmospheric nitrogen deposition across the United States, *Proc. Natl. Acad. Sci.*,
805 113, 4086–4091, <https://doi.org/10.1073/pnas.1515241113>, 2016.

806 Skeffington, R., Whitehead, P., and Abbott, J.: Quantifying uncertainty in critical loads: (B) Acidity mass balance critical loads
807 on a sensitive site, *Water. Air. Soil Pollut.*, 169, 25–46, <https://doi.org/10.1007/s11270-006-2218-9>, 2006.

808 SLCWG: Soil landscapes of Canada version 3.2 [dataset], Soil Landscapes of Canada Working Group. Agriculture and Agri-
809 Food Canada, <https://sis.agr.gc.ca/cansis/nsdb/slc/v3.2/index.html>, 2010.

810 Statistics Canada: Agricultural ecumene boundary file, 2016 Census of Agriculture [dataset], Statistics Canada, Cat. No 92-639-
811 X, <https://www150.statcan.gc.ca/>, 2017.

812 Sverdrup, H. and De Vries, W.: Calculating critical loads for acidity with the simple mass balance method, *Water. Air. Soil*
813 *Pollut.*, 72, 143–162, <https://doi.org/10.1007/BF01257121>, 1994.

814 Sverdrup, H. and Warfvinge, P.: The effect of soil acidification effect on the growth of trees, grass and herbs, as expressed by the
815 $(Ca+ Mg+ K)/Al$ ratio, Reports in ecology and environmental engineering, Lund University Department of Chemical Engineering
816 II, 1993.

817 Tegen, I. and Fung, I.: Contribution to the atmospheric mineral aerosol load from land surface modification, *J. Geophys. Res.*
818 *Atmospheres*, 100, 18707–18726, <https://doi.org/10.1029/95JD02051>, 1995.

819 Tol, P.: Colour schemes, SRON Technical Note, Doc. no. SRON/EPS/TN/09-002, [https://personal.sron.nl/pault/colourschemes.](https://personal.sron.nl/pault/colourschemes.pdf)
820 pdf, 2012.

821 Vandinther, N. and Aherne, J.: Biodiversity-Based Empirical Critical Loads of Nitrogen Deposition in the Athabasca Oil Sands
822 Region, *Nitrogen*, 4, 169–193, <https://doi.org/10.3390/nitrogen4020012>, 2023a.

823 Vandinther, N. and Aherne, J.: Ecological Risks from Atmospheric Deposition of Nitrogen and Sulphur in Jack Pine forests of
824 Northwestern Canada, *Nitrogen*, 4, 102–124, <https://doi.org/10.3390/nitrogen4010008>, 2023b.

825 Whitfield, C. J., Aherne, J., Watmough, S. A., and McDonald, M.: Estimating the sensitivity of forest soils to acid deposition in
826 the Athabasca Oil Sands Region, Alberta, *J. Limnol.*, 69, 201, <https://doi.org/10.4081/jlimnol.2010.s1.201>, 2010.

827 Wilkins, K., Cathcart, H., Hickey, P., Hanley, O., Vintró, L. L., and Aherne, J.: Influence of Precipitation on the Spatial
828 Distribution of ^{210}Pb , ^{7}Be , ^{40}K and ^{137}Cs in Moss, *Pollutants*, 3, 102–113, <https://doi.org/10.3390/pollutants3010009>, 2023.

829 Williston, P., Aherne, J., Watmough, S., Marmorek, D., Hall, A., de la Cueva Bueno, P., Murray, C., Henolson, A., and
830 Laurence, J. A.: Critical levels and loads and the regulation of industrial emissions in northwest British Columbia, Canada,
831 *Atmos. Environ.*, 146, 311–323, <https://doi.org/10.1016/j.atmosenv.2016.08.058>, 2016.

832 Wu, W. and Driscoll, C. T.: Impact of Climate Change on Three-Dimensional Dynamic Critical Load Functions, *Environ. Sci.*
833 *Technol.*, 44, 720–726, <https://doi.org/10.1021/es900890t>, 2010.

834 Zhao, W., Zhao, Y., Ma, M., Chang, M., and Duan, L.: Long-term variability in base cation, sulfur and nitrogen deposition and
835 critical load exceedance of terrestrial ecosystems in China, *Environ. Pollut.*, 289, 117974,
836 <https://doi.org/10.1016/j.envpol.2021.117974>, 2021.

837